

Existence and stability of standing waves for one dimensional NLS with triple power nonlinearities

Fei Liu* Tai-Peng Tsai† Ian Zwieters‡

Abstract

In this note we study analytically and numerically the existence and stability of standing waves for one dimensional nonlinear Schrödinger equations whose nonlinearities are the sum of three powers. Special attention is paid to the curves of non-existence and curves of stability change on the parameter planes.

Contents

1	Introduction	2
2	Preliminaries	5
2.1	Existence	5
2.2	Stability	7
2.3	Sum of positive powers	8
2.4	Double power nonlinearities	9
3	Existence for triple power nonlinearities	10
3.1	Definition and basic properties of existence regions of parameters	10
3.2	Double zeros of the potential function G	11
3.3	Characterization of non-existence regions of parameters	12
3.4	Solutions inside the standing wave homoclinic orbit	14
4	Stability regions of parameters	16
4.1	Limits of the stability functional J near the nonexistence curve	17
4.2	Level sets of the stability functional J and stability regions	18
5	Numerics	21
5.1	Level curves and stability regions	22
5.2	The curve of stability change Γ_{cr} and its minimal point (ω_2, γ_2)	23
5.3	The standing waves	30
6	Appendix: Explicit formulas for standing waves	35
	References	37

*Department of Applied Mathematics, University of Waterloo, Waterloo, ON N2L 3G1, Canada.
feiliu0625@gmail.com

†Department of Mathematics, University of British Columbia, Vancouver, BC V6T 1Z2, Canada.
ttsai@math.ubc.ca.

‡Email: ian.zwieters@gmail.com

1 Introduction

Consider the one dimensional nonlinear Schrödinger equations (NLS) for $u(t, x) : \mathbb{R} \times \mathbb{R} \rightarrow \mathbb{C}$,

$$i\partial_t u + \partial_x^2 u + f(u) = 0, \quad (1.1)$$

with the nonlinearity $f(u) : \mathbb{C} \rightarrow \mathbb{C}$ satisfying $f(u)/u \rightarrow 0$ as $u \rightarrow 0$, and $f(\rho e^{is})e^{-is} = f(\rho) \in \mathbb{R}$ for any $\rho, s \in \mathbb{R}$. A *standing wave* is a solution of (1.1) of the form $u(t, x) = \phi(x)e^{i\omega t}$ for some $\omega \in \mathbb{R}$ and a real-valued *profile* $\phi \in L^2(\mathbb{R})$, which then satisfies

$$\phi'' + f(\phi) = \omega\phi. \quad (1.2)$$

We only consider solutions which decay rapidly at spatial infinity and hence assume $\omega > 0$. The aim of this paper is to examine the existence and stability of standing waves for nonlinearities which are the sum of powers,

$$f(u) = \sum_{j=1}^m a_j |u|^{p_j-1} u, \quad 0 \neq a_j \in \mathbb{R}, \quad 1 < p_1 < \dots < p_m < \infty. \quad (1.3)$$

The cases $m = 1$ and $m = 2$ (single and double power nonlinearities) are well studied and will be reviewed in Section 2. We will focus on $m = 3$ in this paper with $p_j = j + 1$. Thus we consider the triple power nonlinearity

$$f(u) = a_1 |u|u + a_2 |u|^2 u + a_3 |u|^3 u, \quad (1.4)$$

with $a_1 a_2 a_3 \neq 0$. We may also consider other exponents and higher dimensions: A radial standing wave $u(x, t) = \phi(|x|)e^{i\omega t}$ in \mathbb{R}^n satisfies

$$\phi'' + \frac{n-1}{r} \phi' + a_1 |\phi|^{p_1-1} \phi + a_2 |\phi|^{p_2-1} \phi + a_3 |\phi|^{p_3-1} \phi = \omega\phi.$$

We limit ourselves to 1D with nonlinearity (1.4) in this paper.

We now recall known results. The existence and stability of standing wave solutions for general nonlinearities and general dimensions have a large literature. For existence, we refer to Berestycki and Lions [3] and its references. Our Proposition 2.1 is from [3]. The standard references for stability are Grillakis, Shatah, and Strauss [27, 13, 14]. When restricted to one space dimension, one can decide the stability by the sign of a stability functional defined by an integral found by Iliev and Kirchev [16], see Proposition 2.2.

We now consider standing waves for sums of power nonlinearities (1.3). For the single power nonlinearity $f(u) = |u|^{p-1}u$, the solutions are well known, and their stability problem has an extremely large literature and is still very active. Since it is not the concern of this paper, we only refer to the monograph [5] by Cazenave for an introduction.

Consider now a double power nonlinearity, $f(u) = a_1 |u|^{p_1-1}u + a_2 |u|^{p_2-1}u$. In the one dimensional setting, and if at least one of a_j is positive, the standing waves ϕ_ω exist for $\omega \in (0, \omega^*)$ for some $0 < \omega^* \leq \infty$. If both a_1 and a_2 are negative, there is no standing wave. When $2p_1 = p_2 + 1$, explicit formulas for the standing waves are known (see Appendix §6). Their orbital stability is examined by Ohta [24], and extended by Maeda [20]. See Proposition 2.3 for a summary. Note that the case $a_1 < 0 < a_2$ with $p_2 < 5$ is not completely characterized yet. The small frequency case $\omega \ll 1$ has been recently investigated by Fukaya and Hayashi [10] for general dimensions. For space dimension $n \geq 2$, see Fukuizumi [11], Lewin and Nodari [19], and Carles, Klein, and Sparber [4]. For related results, see [12, 1, 2] for the stability for cubic-quintic nonlinearity with an additional delta potential, [17] for

the existence of standing waves for double power nonlinearity and harmonic potential, and [18, 26] for blow up solutions for double power nonlinearities.

We are not aware of any study focused on the triple power nonlinearity, which is the subject of this paper.

Of great interest to us is the co-existence of stable and unstable standing waves for some fixed nonlinearities, with ω being the only parameter. One wonders that, if a solution starts near a unstable standing wave, would it leave the neighborhood of unstable standing waves, and eventually converge to a *stable* standing wave? This is partly motivated by our previous study [22] and [6]. Another motivation is the study of the (in)stability of *critical standing waves*. A standing wave family $\phi_\omega e^{i\omega t}$ may change from being stable to unstable as ω goes across a critical ω_c . It is shown by Comech and Pelinovsky [8] that the critical $\phi_{\omega_c} e^{i\omega_c t}$ is unstable under certain conditions. Their results are extended by Ohta [25] and Maeda [21] under various conditions. These results for NLS are extended to generalized KdV by Comech, Cuccagna, and Pelinovsky [7], and to derivative nonlinear Schrödinger equation by Fukaya [9], Guo, Ning, and Wu [15], and Ning [23]. We hope that, for explicit nonlinearities in one space dimension, one is able to verify those conditions and do more detailed analysis.

We now consider our nonlinearity in more details. To study NLS (1.1) with $f(u)$ given by (1.4), we may let $u(x, t) = kv(\lambda^{-1}x, \lambda^{-2}t)$, $k, \lambda > 0$. Then v satisfies

$$\begin{aligned} i\partial_t v + v_{xx} + \bar{b}|v|v + \bar{c}|v|^2v + \bar{d}|v|^3v &= 0, \\ \bar{b} = a_1k\lambda^2, \quad \bar{c} = a_2k^2\lambda^2, \quad \bar{d} = a_3k^3\lambda^2. \end{aligned}$$

If we choose $k = |a_1/a_3|^{1/2}$ and $\lambda = |a_3/a_1^3|^{1/4}$, then $|\bar{b}| = |\bar{d}| = 1$. Since v and u have the same qualitative properties, we may assume $|a_1| = |a_3| = 1$ without loss of generality. For the rest of this paper, we consider

$$a_1 = \pm 1, \quad a_2 = -\gamma, \quad a_3 = \pm 1, \tag{1.5}$$

and use $\gamma \in \mathbb{R}$ as another parameter in addition to ω . To summarize, our standing wave profile $\phi : \mathbb{R} \rightarrow \mathbb{R}_+$ satisfies

$$\begin{aligned} \phi'' = g(\phi) = \omega\phi - f(\phi), \quad f(\phi) = a_1|\phi|\phi - \gamma|\phi|^2\phi + a_3|\phi|^3\phi, \\ \phi(t) > 0 \quad \forall t \in \mathbb{R}, \quad \lim_{t \rightarrow \pm\infty} \phi(t) = 0, \end{aligned} \tag{1.6}$$

with $a_1, a_3 = \pm 1$. We have two parameters $\omega > 0$ and $\gamma \in \mathbb{R}$, which lie on the half plane $(0, \infty) \times \mathbb{R}$.

We consider 4 cases F*F, F*D, D*F and D*D, where the case F*D means $a_1 = 1$, $a_3 = -1$, and consists of two subcases: FFD means $a_2 > 0$ and FDD means $a_2 < 0$. The remaining cases are similarly defined. The negative sign in front of γ is convenient for the most interesting FDF case. There are 8 combinations of the signs of the three terms. Except the case DDD, the remaining 7 cases have standing waves.

We now present our numerically computed non-existence and stability regions on the parameter half-planes for the 4 cases. See Figures 1–4. The parameter ω is presented in log scale to zoom in the small ω part.

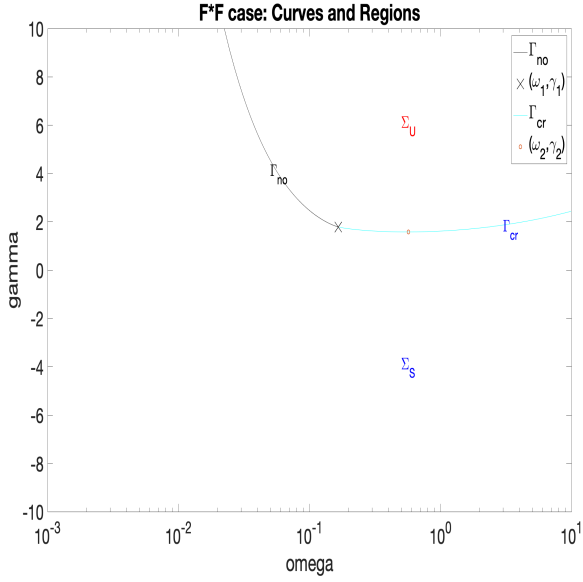


Figure 1: (i) F*F case

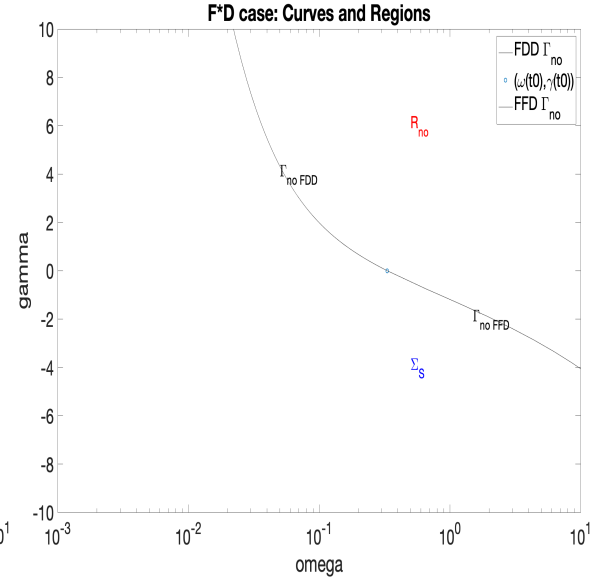


Figure 2: (ii) F*D case

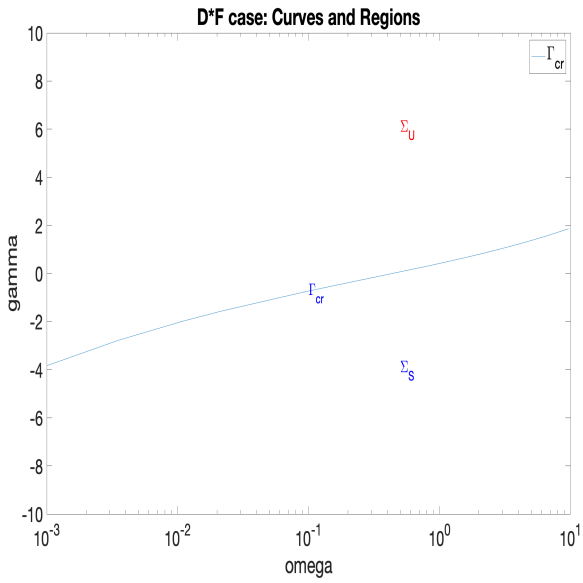


Figure 3: (iii) D*F case

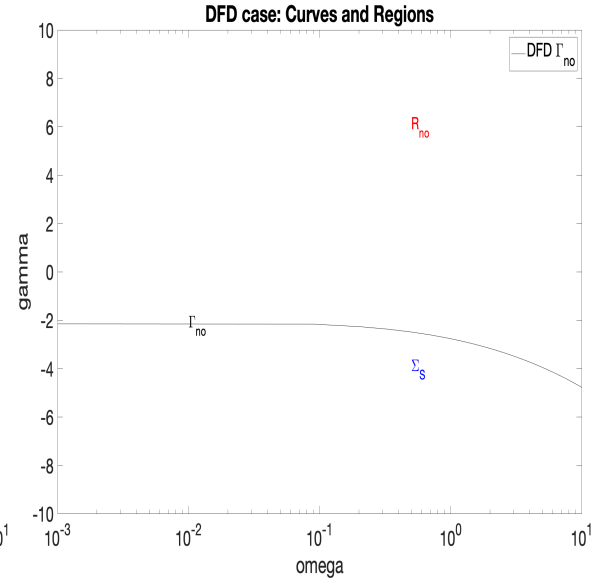


Figure 4: (iv) D*D case

In the figures,

1. R_{no} is the set of (ω, γ) that ϕ does not exist, present in (ii) and (iv);
2. Σ_S is the set of (ω, γ) that ϕ exists and is stable, present in all cases;
3. Σ_U is the set of (ω, γ) that ϕ exists and is unstable, present in (i) and (iii);
4. Γ_{no} is the curve of (ω, γ) that ϕ does not exist, present in (i), (ii) and (iv);
5. Γ_{cr} is the curve of (ω, γ) that ϕ exists and is at threshold of stability, present in (i) and (iii).

The boundary curves Γ_{no} for existence will be analytically computed in Section 3, based on the study of double zeros of the potential function $G(x) = \int_0^x g(s)ds$ for $g(s)$ given in (1.6). In contrast, the curves Γ_{cr} for stability change are computed only numerically, see Section 4.

Among the 4 cases, the F*F case seems the most interesting, as Γ_{no} and Γ_{cr} co-exist and meet at

$$(\omega_1, \gamma_1) := \left(\frac{2\sqrt{5}}{27}, \frac{4}{\sqrt{5}} \right) \approx (0.1656, 1.7889).$$

Moreover, Γ_{cr} has a minimal γ value at (see (5.10))

$$(\omega_2, \gamma_2) \approx (\omega_2^{**}, \gamma_2^{**}) = (0.554837092755109, 1.58170475989899).$$

The pair (ω_1, γ_1) is computed analytically, while (ω_2, γ_2) is only computed numerically. The accuracy of γ_2^{**} is about 10^{-9} , but the accuracy of ω_2^{**} is about 10^{-4} , much larger. See §5.2.

We now explain the structure of the paper. In Section 2, we recall the general existence and stability results, and the known results for double power nonlinearities.

In Section 3, we analyze the existence for the triple power nonlinearity (1.4)-(1.5) by studying the double zeros of the potential function $G(x; \omega, \gamma)$. We characterize the existence regions and their boundary Γ_{no} . We also study solutions inside the standing wave homoclinic orbit in Subsection 3.4.

In Section 4, we study the stability regions by studying the stability function $J(\omega, \gamma)$. We study analytically the limits of $J(\omega, \gamma)$ as (ω, γ) approaches the non-existence curve Γ_{no} from different sides in Subsection 4.1, and characterize the stability regions for the four cases using the level sets of J in Subsection 4.2.

In Section 5 we discuss our numerical methods and observations. In Subsection 5.1, we describe the computations of the level curves of the stability functional $J(\omega, \gamma)$ and the stability regions for the four cases. In Subsection 5.2, we describe the computation of the curve of stability change Γ_{cr} and its minimal point (ω_2, γ_2) in the F*F case. In Subsection 5.3, we describe the 3 methods that we use for computing the standing wave $\phi_{\omega, \gamma}$.

In Appendix Section 6, we give alternative explicit formulas for the standing waves of (6.3) for double power nonlinearities with $2p_1 = p_2 + 1$.

2 Preliminaries

In this section we recall some general results for bounded solutions $u : \mathbb{R} \rightarrow \mathbb{R}$ of

$$u'' = g(u) = \omega u - f(u), \quad \omega > 0, \quad \lim_{u \rightarrow 0} \frac{f(u)}{u} = 0. \quad (2.1)$$

2.1 Existence

The following is a general existence result.

Proposition 2.1 (Existence [3]). *Let $g \in C(\mathbb{R}; \mathbb{R})$ be a locally Lipschitz continuous function with $g(0) = 0$ and let $G(t) = \int_0^t g(s)ds$. A necessary and sufficient condition for the existence of a solution ϕ of the problem*

$$\phi \in C^2(\mathbb{R}), \quad \lim_{t \rightarrow \pm\infty} \phi(t) = 0, \quad \phi(0) > 0, \quad (2.2)$$

$$\phi'' = g(\phi), \quad (2.3)$$

is that

$$\phi_0 = \inf\{t > 0 : G(t) = 0\} \text{ exists, } \phi_0 > 0, \quad g(\phi_0) < 0. \quad (2.4)$$

For the special case (2.1), the existence can be derived directly from the phase plane analysis for (2.3) without use of Proposition 2.1. We now describe it. The corresponding planar first order system for (2.3) is, with $x = \phi$ and $y = \dot{\phi}$,

$$\dot{x} = y, \quad \dot{y} = g(x). \quad (2.5)$$

Every solution moves on a level curve of the total energy

$$E(x, y) = \frac{1}{2}y^2 - G(x) = \frac{1}{2}y^2 - \frac{\omega}{2}x^2 + F(x),$$

where $F(x) = \int_0^x f(t) dt$. Assume that G has a smallest positive zero $\phi_0 > 0$, $G(\phi_0) = 0$. We have $g(\phi_0) \leq 0$ because $G(x) > 0$ for $0 < x < \phi_0$. As $E(x, 0) = -G(x) < 0$ for small $x > 0$, by continuity,

$$E(x, 0) = -G(x) < 0, \quad 0 < x < \phi_0.$$

For the single power nonlinearity $f(u) = |u|^{p-1}u$ and $g(u) = \omega u - f(u)$, the solution passing through $(x, y) = (\alpha, 0)$ with $0 < \alpha < \phi_0$ is either a fixed point or a periodic orbit. But this is not true for general $f(u)$. See Lemma 3.6 and Examples 3.7–3.8 for the triple power case.

The nature of the solution passing through $(x, y) = (\phi_0, 0)$ depends on whether $g(\phi_0) = 0$. Let Ω denote the connected component of the sublevel set $E < 0$ that contains the open line segment from $(0, 0)$ to $(\phi_0, 0)$. It is bounded, and $E = 0$ on its boundary $\partial\Omega$. We assume $\partial\Omega$ is a nice curve lying in between $0 \leq x \leq \phi_0$. Its fixed point(s) lie on the x -axis since $\dot{x} = y \neq 0$ if $y \neq 0$.

1. If $g(\phi_0) = 0$: $(\phi_0, 0)$ is a fixed point of (2.5). The upper branch of $\partial\Omega$ in the first quadrant is a heteroclinic orbit from $(0, 0)$ to $(\phi_0, 0)$.
2. If $g(\phi_0) < 0$: $(\phi_0, 0)$ is not a fixed point. The curve $\partial\Omega$ is a homoclinic orbit from $(0, 0)$ to $(0, 0)$ passing through $(\phi_0, 0)$. The x -component of this orbit is always positive.

Formally the solution passing $(\phi_0, 0)$ satisfies $E = \frac{1}{2}y^2 - G(x) = 0$. Suppose $(\phi_0, 0) = (x(0), y(0))$. Then the branch in the fourth quadrant (corresponding to $0 < t < \infty$) satisfies

$$\frac{dx}{dt} = -\sqrt{2G(x)}, \quad dt = -\frac{dx}{\sqrt{2G(x)}}. \quad (2.6)$$

If $x(0) = \phi_0$ and $x(t) = \phi$, then

$$t = -\int_{\phi_0}^{\phi} \frac{dx}{\sqrt{2G(x)}}. \quad (2.7)$$

If $g(\phi_0) = 0$, then ϕ_0 is a double zero of G , and the integral (2.7) is not integrable. This agrees with the fact that $(\phi_0, 0)$ is a fixed point. If $g(\phi_0) < 0$, then (2.7) is a well-defined improper integral. The integrand is positive for any $x \in (0, \phi_0)$, and hence the integral is well-defined. As $x \rightarrow 0_+$, $\sqrt{2G(x)} \sim \sqrt{\omega}x$. Hence $t \rightarrow \infty$ as $\phi \rightarrow 0_+$. The inverse function of the integral function (2.7) is our desired solution $\phi(t) = \phi_\omega(t)$.

We may now treat ω as a parameter and denote $\phi = \phi_\omega$. The set of ω for which ϕ_ω exists is open because the existence condition (2.4) that ϕ_0 is that first zero of G and that $g(\phi_0) < 0$ are preserved under small perturbations in ω .

2.2 Stability

The *orbit* of a standing wave $\phi e^{i\omega t}$ is the set obtained from it by translation and phase shift,

$$\mathcal{O}_\phi = \{e^{i\eta}\phi(\cdot - \xi) : (\xi, \eta) \in \mathbb{R}^2\}.$$

The distance of u to this orbit of ϕ is

$$\text{dist}(u, \mathcal{O}_\phi) = \inf_{(\xi, \eta) \in \mathbb{R}^2} \|u - e^{i\eta}\phi(\cdot - \xi)\|_{H^1(\mathbb{R})}.$$

We say a standing wave $\phi e^{i\omega t}$ is *orbitally stable* if

$$\forall \varepsilon > 0, \exists \delta > 0, \text{ s.t. } \text{dist}(u(0), \mathcal{O}_\phi) < \delta \Rightarrow \text{dist}(u(t), \mathcal{O}_\phi) < \varepsilon \quad \forall t \geq 0,$$

where $u(t)$ is the solution of (1.1) with initial data $u(0)$. This definition falls in the general framework of [14], and differs from [27, 13] since the orbit contains translations. We may remove the translations from \mathcal{O}_ϕ if we restrict our perturbations to even perturbations so that the solutions do not move. For general (non-even) perturbations, the solutions may get boost from the perturbations and start to move, and hence we need to contain translations in \mathcal{O}_ϕ . For example, we may get a traveling wave by the Galilean transformation for $v \neq 0$,

$$u(x, t) = \phi_\omega(x - vt)e^{i(\omega t + vx/2 - tv^2/4)}.$$

We prepare a few definitions before we state an orbital stability result. For a family of standing waves ϕ_ω , $\omega \in (\omega_a, \omega_b)$, denote

$$d(\omega) = E(\phi_\omega) + \omega Q(\phi_\omega),$$

where

$$E(u) = \int_{\mathbb{R}} |u_x|^2 - 2F(u) dx, \quad Q(u) = \int_{\mathbb{R}} |u|^2 dx.$$

Then, assuming enough regularity of f , $d(\omega)$ is C^2 and

$$d'(\omega) = Q(\phi_\omega).$$

Following [16], we denote for $s \geq 0$

$$\begin{aligned} f(s) &= -f_1(s^2)s, \quad F_1(s) = \int_0^s f_1(t)dt = -2F(\sqrt{s}), \\ U(s) &= \omega s + F_1(s) = \omega s - 2F(\sqrt{s}) = 2G(\sqrt{s}), \quad U'(s) = \frac{g(\sqrt{s})}{\sqrt{s}}. \end{aligned} \quad (2.8)$$

(f_1 and F_1 are denoted as f and g in [16].) The existence condition (2.4) is equivalent to (with $a = \phi_0^2$)

$$\exists a \in (0, \infty) \text{ such that } U(a) = 0, \quad U'(a) < 0, \quad U(s) > 0 \quad (0 < s < a). \quad (2.9)$$

The following is an orbital stability result by Iliev and Kirchev [16].

Proposition 2.2 (Orbital stability [16]). *Suppose $f(u)$ is such that (1.1) is locally wellposed in $H^2(\mathbb{R})$, there is a constant $A > 0$ such that $f_1(s) \in C^0[0, A] \cap C^1(0, A)$, $sf_1'(s) \rightarrow 0$ as $s \rightarrow 0$, and (2.9) is satisfied with $a < A$. If $d''(\omega) > 0$, then $\phi_\omega e^{i\omega t}$ is orbitally stable. If $d''(\omega) < 0$, then $\phi_\omega e^{i\omega t}$ is orbitally unstable. Furthermore,*

$$d''(\omega) = \frac{d}{d\omega} \int \phi_\omega^2(x) dx = \frac{-1}{2U'(a)} \int_0^a \left(3 + \frac{as[f_1(a) - f_1(s)]}{aF_1(s) - sF_1(a)} \right) \left(\frac{s}{U(s)} \right)^{1/2} ds. \quad (2.10)$$

The last formula is [16, Lemma 6]. Note that $f_1(a) - f_1(s) = U'(a) - U'(s)$ and

$$aF_1(s) - sF_1(a) = a(U(s) - \omega s) - s(U(a) - \omega a) = aU(s).$$

Hence

$$d''(\omega) = \frac{-1}{2U'(a)} \int_0^a \left(3 + \frac{s(U'(a) - U'(s))}{U(s)} \right) \left(\frac{s}{U(s)} \right)^{1/2} ds. \quad (2.11)$$

Changing variable $s = a\sigma$ and relabeling σ as s , we get the form we use in MATLAB:

$$d''(\omega) = \frac{-a^{1.5}}{2U'(a)} \int_0^1 \left(3 + \frac{as(U'(a) - U'(as))}{U(as)} \right) \frac{\sqrt{s}}{\sqrt{U(as)}} ds. \quad (2.12)$$

This formula is convenient for numerics since it has a fixed domain $(0, 1)$ and we only need to compute the vectors $U_k = U(ak/N)$ and $V_k = U'(ak/N)$, $0 \leq k \leq N$, and do not need to compute f_1 or F_1 .

If we make the natural change of variables $s = x^2$ (with $x = \phi_\omega(t)$), using (2.8) and $a = \phi_0^2$, we get

$$d''(\omega) = \frac{-\sqrt{2}}{4g(\phi_0)} \int_0^{\phi_0} \left\{ \frac{6\phi_0}{\sqrt{G(x)}} + \frac{x[xg(\phi_0) - \phi_0g(x)]}{\sqrt{G(x)}^3} \right\} x^2 dx. \quad (2.13)$$

Note that we are free to add into the integral of (2.13)

$$0 = \int_0^{\phi_0} \frac{d}{dx} \left(\frac{2A(x)}{\sqrt{G(x)}} \right) dx = \int_0^{\phi_0} \left(\frac{2A'(x)}{\sqrt{G(x)}} - \frac{A(x)g(x)}{\sqrt{G(x)}^3} \right) dx \quad (2.14)$$

for any $A(x) \in C^1([0, \phi_0])$ with $A(0) = A'(\phi_0) = A(\phi_0) = 0$. For example, the choice $A(x) = -\phi_0 x^3$ does not satisfy $A(\phi_0) = 0$, while the choices $A(x) = x^4 - \phi_0 x^3$ and $A(x) = \phi_0^2 x^2 - \phi_0 x^3$ are valid and give us

$$d''(\omega) = \frac{-\sqrt{2}}{4g(\phi_0)} \int_0^{\phi_0} \frac{8x^3 G(x) + x^4 g(\phi_0) - x^4 g(x)}{\sqrt{G(x)}^3} dx \quad (2.15)$$

and

$$d''(\omega) = \frac{-\sqrt{2}}{4g(\phi_0)} \int_0^{\phi_0} \frac{4\phi_0^2 x G(x) + x^4 g(\phi_0) - \phi_0^2 x^2 g(x)}{\sqrt{G(x)}^3} dx. \quad (2.16)$$

2.3 Sum of positive powers

We now consider the special case that $f(u)$ is a sum of m positive power nonlinearities, given as in (1.3), with all coefficients $a_i > 0$.

In the classical case $m = 1$ and $f(u) = a_1 |u|^{p_1 - 1} u$, a lot is known: We need $a_1 > 0$ to ensure the existence. In this case ϕ_ω exist for all ω , and indeed are the rescaling of each other. It is well known that they are stable if $p_1 < 5$ and unstable if $5 \leq p_1$. This result follows from Proposition 2.2 if $p_1 \neq 5$ (see the argument for $m > 1$ case below), and needs extra work if $p_1 = 5$. See e.g. [5].

When $m > 1$, $f(u)$ is given by (1.3), and all a_1, \dots, a_m are positive, we have

$$G(u) = \frac{\omega}{2} |u|^2 - F(u), \quad F(u) = \sum_{k=1}^m \frac{a_k}{p+1} |u|^{p+1}.$$

It clearly has a first positive zero ϕ_0 . Moreover,

$$\frac{1}{2}\phi_0 g(\phi_0) = \frac{\omega}{2}\phi_0^2 - \sum_{k=1}^m \frac{a_k}{2}\phi_0^{p_k+1} < G(\phi_0) = 0.$$

Thus $g(\phi_0) < 0$. By Proposition 2.1, the family of standing waves ϕ_ω exist for all $0 < \omega < \infty$.

For their stability, rewrite (2.11) as

$$d''(\omega) = \frac{-1}{2U'(a)} \int_0^a I(s) \left(\frac{s}{U(s)} \right)^{\frac{3}{2}} ds, \quad I(s) = \frac{3U(s)}{s} + f_1(a) - f_1(s). \quad (2.17)$$

Using $U(s)/s = 2G(\sqrt{s})/s = \omega - \sum_{k=1}^m \frac{2a_k}{p_k+1} s^{\sigma_k}$, where $\sigma_k = \frac{p_k-1}{2}$, $U(a) = 0$ hence $\omega = \sum_{k=1}^m \frac{2a_k}{p_k+1} a^{\sigma_k}$, and $f_1(s) = -f(\sqrt{s})/\sqrt{s} = -\sum_{k=1}^m a_k s^{\frac{p_k-1}{2}}$, we get

$$\begin{aligned} I(s) &= \frac{3U(s)}{s} + f_1(a) - f_1(s) \\ &= \sum_k \frac{6a_k}{p_k+1} (a^{\sigma_k} - s^{\sigma_k}) - \sum_k a_k (a^{\sigma_k} - s^{\sigma_k}) \\ &= \sum_k \frac{a_k(5-p_k)}{p_k+1} (a^{\sigma_k} - s^{\sigma_k}). \end{aligned}$$

Since $m > 1$, $I(s) > 0$ for $0 < s < a$ if $p_m \leq 5$. In this case, ϕ_ω for all ω are orbital stable by Proposition 2.2 and (2.17). On the other hand, if $p_1 \geq 5$, $I(s) < 0$ for $0 < s < a$, hence ϕ_ω for all ω are orbital unstable. The intermediate cases $p_1 < 5 < p_m$ are more subtle.

2.4 Double power nonlinearities

When $m = 2$ and f is a double power nonlinearity,

$$f(u) = a_1|u|^{p_1-1}u + a_2|u|^{p_2-1}u, \quad 1 < p_1 < p_2 < \infty, \quad a_1 a_2 \neq 0, \quad (2.18)$$

and if at least one of a_j is positive, the standing waves ϕ_ω exist for $\omega \in (0, \omega^*)$ for some $0 < \omega^* \leq \infty$. If both a_1 and a_2 are negative, there is no standing wave. Their stability is examined by Ohta [24], and extended by Maeda [20]. To present their results in a compact form, we make the following

Definition. The family $\{\phi_\omega\}_{0 < \omega < \omega^*}$ is of type SU if there exist $0 < \omega_1 < \omega^*$ so that ϕ_ω is stable for $\omega \in (0, \omega_1)$, and unstable for $\omega \in (\omega_1, \omega^*)$. It is of type U?S if there exist $0 < \omega_1 < \omega_2 < \omega^*$ so that ϕ_ω is unstable for $\omega \in (0, \omega_1)$, unknown for $\omega \in (\omega_1, \omega_2)$, and stable for $\omega \in (\omega_2, \omega^*)$. There is no assertion at ω_1 and ω_2 . Other types are defined similarly.

We summarize the results of [24, 20] in the following.

Proposition 2.3. *Let $f(u)$ be of the form (2.18). We consider the stability type of the family $\{\phi_\omega\}_{0 < \omega < \omega^*}$ in three groups:*

(focusing-focusing, FF) *Let $a_1, a_2 > 0$. Then $\omega^* = \infty$.*

(a) *If $p_2 \leq 5$, it is of type S.*

(b) *If $p_1 \geq 5$, it is of type U.*

(c) *If $p_1 < 5 < p_2$, it is of type SU.*

(focusing-defocusing, FD) *Let $a_1 > 0, a_2 < 0$. Then $\omega^* < \infty$.*

(a) *If $p_1 \leq 5$, it is of type S.*

(b) If $p_1 > 5$, it is of type US.

(defocusing-focusing, DF) Let $a_1 < 0$, $a_2 > 0$. Then $\omega^* = \infty$.

(a) If $p_2 \geq 5$, it is of type U.

(b) If $p_2 < 5$, it is of type ?S.

If $p_2 < 5$ and $p_1 + p_2 > 6$, it is of type U?S.

If $p_2 < 5$, $p_1 + p_2 > 6$, and $7/3 < p_1$, it is of type US.

If $p_1 = 2$ and $p_2 = 3$, it is of type S.

Note that the case (DF)-(b) is not completely decided. However, it is conjectured that the stability change occurs at most once [20, p.265]. The instability of standing waves with small frequency ω in the DF case has been recently investigated by Fukaya and Hayashi [10] for general dimensions. For dimension 1, standing waves with sufficiently small ω are unstable if $1 < p_1 < p_2 < 5$ and $(p_1 + 3)(p_2 + 3) > 32$.

Note that, for double power nonlinearity with $2p_1 = p_2 + 1$, explicit formulas for the standing waves are known. We will give a new formulation which gives the standing waves for all FF, FD and DF cases in one single formula in Appendix §6.

3 Existence for triple power nonlinearities

In this section, we study the existence of the standing wave profile $\phi : \mathbb{R} \rightarrow \mathbb{R}_+$ satisfying (1.6) with triple power nonlinearity for parameters $\omega > 0$ and $\gamma \in \mathbb{R}$, that is,

$$\begin{aligned} \phi'' &= g(\phi) = \omega\phi - f(\phi), & f(\phi) &= a_1|\phi|\phi - \gamma|\phi|^2\phi + a_3|\phi|^3\phi, \\ \phi(t) &> 0 \quad \forall t \in \mathbb{R}, & \lim_{t \rightarrow \pm\infty} \phi(t) &= 0, \end{aligned}$$

for the four cases $a_1, a_3 = \pm 1$. Recall $G(x) = \int_0^x g$. For our special choice of f ,

$$G(x) = \frac{\omega}{2}x^2 - \frac{a_1}{3}|x|^3 + \frac{\gamma}{4}x^4 - \frac{a_3}{5}|x|^5, \quad (x \in \mathbb{R}). \quad (3.1)$$

3.1 Definition and basic properties of existence regions of parameters

By Section 2.1, the standing wave profile ϕ exists if and only if that

(E1) the first positive zero ϕ_0 of $G(x)$ exists, and

(E2) $g(\phi_0) < 0$.

(E1) fails if $G(x) > 0$ for all $x > 0$. When (E1) is valid, (E2) fails if ϕ_0 is a double zero of G , $g(\phi_0) = 0$.

Condition (E2) is preserved under small perturbations of ω and γ . Condition (E1) by itself is not so, because the first positive zero may disappear or jump under perturbations of ω and γ . However, when any of these happens, it is necessary that $g(\phi_0) = 0$, violating (E2). We formulate this as a lemma.

Lemma 3.1. *Suppose (E1) and (E2) are valid at $(\omega_0, \gamma_0) \in \mathbb{R}_+ \times \mathbb{R}$. Then it is valid in a small neighborhood of (ω_0, γ_0) . Moreover, the map $(\omega, \gamma) \mapsto \phi_0(\omega, \gamma)$ is continuous in the neighborhood.*

Proof. Let ϕ_0 be the first zero of G at (ω_0, γ_0) . Let $H(x, \omega, \gamma) = \frac{\omega}{2}x^2 - \frac{a_1}{3}x^3 + \frac{\gamma}{4}x^4 - \frac{a_3}{5}x^5$. We have $H(\phi_0, \omega_0, \gamma_0) = 0$ and $H_x(\phi_0, \omega_0, \gamma_0) < 0$. By the implicit function theorem, there is a continuous map $X(\omega, \gamma)$ in a small neighborhood of (ω_0, γ_0) such that $H(X(\omega, \gamma), \omega, \gamma) = 0$ and $X(\omega_0, \gamma_0) = \phi_0$. We also have $H_x(X(\omega, \gamma), \omega, \gamma) < 0$ by continuity. We may choose a smaller neighborhood to ensure that $X(\omega, \gamma)$ remains the first positive zero. \square

For each of the 4 cases $a_1, a_3 = \pm 1$, we denote by R_{ex} the subset of parameters $(\omega, \gamma) \in \mathbb{R}_+ \times \mathbb{R}$ for which the standing wave profile ϕ exists. That is, both (E1) and (E2) are valid. By Lemma 3.1, R_{ex} is an open subset of $\mathbb{R}_+ \times \mathbb{R}$. Let R_{no} be the complement of R_{ex} . It is a closed subset of $\mathbb{R}_+ \times \mathbb{R}$. Let Γ_{no} be the boundary of R_{no} in $\mathbb{R}_+ \times \mathbb{R}$.

Lemma 3.2. *Consider the first positive zero ϕ_0 of G as a function of $(\omega, \gamma) \in R_{\text{ex}}$. It is continuously differentiable and $\frac{\partial \phi_0}{\partial \omega} > 0$ and $\frac{\partial \phi_0}{\partial \gamma} > 0$ for all $(\omega, \gamma) \in R_{\text{ex}}$ and for all 4 cases.*

Proof. Let $H(x, \omega, \gamma) = \frac{\omega}{2}x^2 - \frac{a_1}{3}x^3 + \frac{\gamma}{4}x^4 - \frac{a_3}{5}x^5$. We have $H(\phi_0(\omega, \gamma), \omega, \gamma) = 0$ and $g(\phi_0(\omega, \gamma)) < 0$. Hence

$$0 = \partial_\omega H(\phi_0(\omega, \gamma), \omega, \gamma) = \frac{1}{2}\phi_0^2 + g(\phi_0)\frac{\partial \phi_0}{\partial \omega}, \quad 0 = \partial_\gamma H(\phi_0(\omega, \gamma), \omega, \gamma) = \frac{1}{4}\phi_0^4 + g(\phi_0)\frac{\partial \phi_0}{\partial \gamma}.$$

Thus $\frac{\partial \phi_0}{\partial \omega} = \frac{\phi_0^2}{-2g(\phi_0)} > 0$ and $\frac{\partial \phi_0}{\partial \gamma} = \frac{\phi_0^4}{-4g(\phi_0)} > 0$. \square

Lemma 3.3. *At any $(\omega_0, \gamma_0) \in \Gamma_{\text{no}}$, (E1) is valid and (E2) fails. That is, the first positive zero of G at (ω_0, γ_0) exists and is a double zero.*

Proof. Choose $(\omega_k, \gamma_k) \in R_{\text{ex}}$, $k \in \mathbb{N}$, with $(\omega_k, \gamma_k) \rightarrow (\omega_0, \gamma_0)$ as $k \rightarrow \infty$. Let $\phi_0^k = \phi_0(\omega_k, \gamma_k)$, their first positive zero of G . Since

$$\frac{\omega_k}{2} - \frac{a_1}{3}x + \frac{\gamma_k}{4}x^2 - \frac{a_3}{5}x^3 = 0, \quad x = \phi_0^k,$$

ϕ_0^k is uniformed bounded away from zero and infinity. There is a subsequence, still denoted as ϕ_0^k , that converges to some finite $x_0 > 0$. Taking limits of $H(\phi_0^k, \omega_k, \gamma_k) = 0$, we get $H(x_0, \omega_0, \gamma_0) = 0$. Thus G has a positive zero x_0 at (ω_0, γ_0) and (E1) is valid. By assumption, (E2) fails. Either x_0 is a double zero, or the first positive zero ϕ_0 is less than x_0 . In the latter case, $\phi_0, H(\phi_0, \omega_k, \gamma_k) > 0$ and $\lim_{k \rightarrow \infty} H(\phi_0, \omega_k, \gamma_k) = 0$. Hence ϕ_0 is a double zero. \square

3.2 Double zeros of the potential function G

Suppose (E1) is valid so that G has a positive zero. Then (E2) is valid if and only if the first positive zero of G is not a double zero. Let us now consider all positive double zeros t of G (not necessarily the first positive zero),

$$G(t) = 0, \quad G'(t) = g(t) = 0, \quad t > 0.$$

They correspond to fixed points $(t, 0)$ of (2.5) with zero energy, $E(t, 0) = 0$. Since $G(x)$ is a polynomial of degree 5 and both $x = 0$ and $x = t$ are its double zeros,

$$G(x) = -\frac{a_3}{5}x^2(x-t)^2(x-x_0) \tag{3.2}$$

for some $x_0 \in \mathbb{R}$, $x_0 \neq 0$. Thus for every (ω, γ) there is at most one positive double zero t . When there is one, solving $2G(t)/t^2 = g(t)/t = 0$ using (3.1), we get

$$\omega = a_1 \frac{t}{3} - a_3 \frac{1}{5}t^3, \quad \gamma = a_1 \frac{2}{3t} + a_3 \frac{6}{5}t, \quad x_0 = \frac{5\omega}{2a_3 t^2} = \frac{5a_1}{6a_3 t} - \frac{1}{2}t. \tag{3.3}$$

This gives a candidate curve of parameters for nonexistence. The requirement $\omega > 0$ gives

$$\frac{5}{3}a_1 > a_3 t^2, \quad a_3 x_0 > 0. \tag{3.4}$$

If $x_0 \notin (0, t)$, the double zero t is the first positive zero, and ϕ_ω does not exist. When $x_0 \in (0, t)$, then x_0 is the first positive zero and $G'(x_0) < 0$. Thus ϕ_ω exists with $\phi_\omega(0) = x_0$.

Note that, whenever $d\omega/dt \neq 0$,

$$\frac{d\gamma}{d\omega} = \frac{d\gamma/dt}{d\omega/dt} = -\frac{2}{t^2} < 0. \tag{3.5}$$

3.3 Characterization of non-existence regions of parameters

We now identify the non-existence curve Γ_{no} and non-existence region R_{no} for each of the four cases $a_1, a_3 = \pm 1$.

Theorem 3.4 (Characterization of non-existence regions). *The non-existence curve Γ_{no} and non-existence region R_{no} of parameters $(\omega, \gamma) \in \mathbb{R}_+ \times \mathbb{R}$ for each of the four cases are:*

1. *F*F case $a_1 = a_3 = 1$: The curve $R_{\text{no}} = \Gamma_{\text{no}}$ is given by*

$$\omega = \frac{t}{3} - \frac{1}{5}t^3, \quad \gamma = \frac{2}{3t} + \frac{6}{5}t, \quad 0 < t \leq \frac{\sqrt{5}}{3}. \quad (3.6)$$

We have $(\omega, \gamma) \rightarrow (0, \infty)$ as $t \rightarrow 0_+$ and $(\omega, \gamma) = (\omega_1, \gamma_1) = (\frac{2\sqrt{5}}{27}, \frac{4\sqrt{5}}{5})$ as $t = \frac{\sqrt{5}}{3}$.

2. *F*D case $a_1 = 1 = -a_3$: R_{no} is the set on and above the curve Γ_{no} given by*

$$\omega = \frac{t}{3} + \frac{1}{5}t^3, \quad \gamma = \frac{2}{3t} - \frac{6}{5}t, \quad 0 < t < \infty. \quad (3.7)$$

We have $(\omega, \gamma) \rightarrow (0, \infty)$ as $t \rightarrow 0_+$ and $(\omega, \gamma) \rightarrow (\infty, -\infty)$ as $t \rightarrow \infty$.

3. *D*F case $a_3 = 1 = -a_1$: Both R_{no} and Γ_{no} are empty.*

4. *D*D case $a_1 = a_3 = -1$: R_{no} is the set on and above the curve Γ_{no} given by*

$$\omega = -\frac{t}{3} + \frac{1}{5}t^3, \quad \gamma = -\frac{2}{3t} - \frac{6}{5}t, \quad \sqrt{\frac{5}{3}} < t < \infty. \quad (3.8)$$

We have $(\omega, \gamma) \rightarrow (0, -\frac{8\sqrt{15}}{15})$ as $t \rightarrow \sqrt{\frac{5}{3}}+$ and $(\omega, \gamma) \rightarrow (\infty, -\infty)$ as $t \rightarrow \infty$.

Whenever Γ_{no} exists (cases 1, 2, 4), it has a negative slope everywhere on the curve.

Note that, in the last D*D case, $\frac{8\sqrt{15}}{15} \approx 2.06559$, which agrees with Figure 4.

Proof. By Lemma 3.3, any $(\omega, \gamma) \in \Gamma_{\text{no}}$ must have a first positive zero t which is a double zero. By §3.2, (ω, γ) is given by (3.3). The last statement of negative slope follows from (3.5).

1. F*F case $a_1 = a_3 = 1$. Since $G(0+) > 0$ and $G(x) < 0$ for $x \gg 1$, there is always a solution to $G(x) = 0$, and (E1) is valid for every (ω, γ) . When a positive zero t of G is a double zero, by (3.3) and (3.4),

$$\omega = \frac{t}{3} - \frac{1}{5}t^3, \quad \gamma = \frac{2}{3t} + \frac{6}{5}t, \quad x_0 = \frac{5}{6t} - \frac{1}{2}t > 0, \quad 0 < t < \sqrt{\frac{5}{3}}.$$

For (E2) to fail, we need $x_0 \geq t$, i.e. $t \leq \frac{\sqrt{5}}{3}$. Thus $R_{\text{no}} = \Gamma_{\text{no}}$ is parametrized by the above formula with $0 < t \leq \frac{\sqrt{5}}{3}$. In the interior of this interval, $dw/dt > 0$ and $d\gamma/dt < 0$.

2. F*D case $a_1 = 1 = -a_3$: Since $G(0+) > 0$ and $G(x) > 0$ for $x \gg 1$, for each fixed $\omega > 0$, the function $f(\gamma) = \inf_{x>0} G(x)$ is continuous and nondecreasing in γ and at a minimal $\gamma = \gamma_0(\omega)$ we have $f(\gamma_0(\omega)) = 0$. At this γ , G has a double zero. The curve $\gamma = \gamma_0(\omega)$ describes Γ_0 . The first positive zero of G exists if and only if $\gamma \leq \gamma_0(\omega)$, i.e., (ω, γ) is on or below Γ_{no} . When a positive zero t of G is a double zero, by (3.3) and (3.4),

$$\omega = \frac{t}{3} + \frac{1}{5}t^3, \quad \gamma = \frac{2}{3t} - \frac{6}{5}t, \quad x_0 = -\frac{5}{6t} - \frac{1}{2}t < 0, \quad 0 < t < \infty.$$

As $x_0 < 0$, t is always the first positive zero of G . Thus Γ_{no} is parametrized by the above formula with $0 < t < \infty$. In this interval, $dw/dt > 0$ and $d\gamma/dt < 0$.

3. D*F case $a_3 = 1 = -a_1$: Since $G(0+) > 0$ and $G(x) < 0$ for $x \gg 1$, there is always a solution to $G(x) = 0$, and (E1) is valid for every (ω, γ) . When a positive zero t of G is a double zero, by (3.3),

$$\omega = -\frac{t}{3} - \frac{1}{5}t^3, \quad \gamma = -\frac{2}{3t} + \frac{6}{5}t.$$

But there is no $t > 0$ such that $\omega(t) > 0$. Thus (E2) is valid for every (ω, γ) , and R_{ex} is the entire $\mathbb{R}_+ \times \mathbb{R}$.

4. D*D case $a_1 = a_3 = -1$. Since $G(0+) > 0$ and $G(x) > 0$ for $x \gg 1$, for each fixed $\omega > 0$, the function $f(\gamma) = \inf_{x>0} G(x)$ is continuous and nondecreasing in γ and at a minimal $\gamma = \gamma_0(\omega)$ we have $f(\gamma_0(\omega)) = 0$. At this γ , G has a double zero. The curve $\gamma = \gamma_0(\omega)$ describes Γ_0 . The first positive zero of G exists if and only if $\gamma \leq \gamma_0(\omega)$, i.e., (ω, γ) is on or below Γ_{no} . When a positive zero t of G is a double zero, by (3.3) and (3.4),

$$\omega = -\frac{t}{3} + \frac{1}{5}t^3, \quad \gamma = -\frac{2}{3t} - \frac{6}{5}t, \quad x_0 = \frac{5}{6t} - \frac{1}{2}t < 0, \quad \sqrt{\frac{5}{3}} < t < \infty.$$

As $x_0 < 0$, t is always the first positive zero of G . Thus Γ_{no} is parametrized by the above formula with $\sqrt{\frac{5}{3}} < t < \infty$. In this interval, $dw/dt > 0$ and $d\gamma/dt < 0$. \square

Among the four cases, F*F is the most interesting, with standing waves on both sides of Γ_{no} . Note that at the end point of Γ_{no} ,

$$(\omega_1, \gamma_1) = \left(\frac{2\sqrt{5}}{27}, \frac{4\sqrt{5}}{5} \right) \approx (0.1656, 1.7889), \quad t = \frac{\sqrt{5}}{3} \approx 0.7454, \quad (3.9)$$

the first positive zero $t = \frac{\sqrt{5}}{3}$ is a triple zero of G .

Lemma 3.5. *In all cases (F*F, F*D, D*D) when Γ_{no} exists, for any $(\omega_0, \gamma_0) = (\omega(t), \gamma(t))$ given by (3.3) on Γ_{no} , we have*

$$\lim_{\omega \rightarrow \omega_0^-, \gamma \rightarrow \gamma_0^-} \phi_0(\omega, \gamma) = t.$$

*In the F*F case, we also have*

$$\lim_{\omega \rightarrow \omega_0^+, \gamma \rightarrow \gamma_0^+} \phi_0(\omega, \gamma) = x_0 = \frac{5}{6t} - \frac{1}{2}t, \quad x_0 \geq t,$$

with $x_0 = t$ only at (ω_1, γ_1) with $t = \frac{\sqrt{5}}{3}$.

Note that the limits are taken through $(\omega, \gamma) \in R_{\text{ex}}$ and exist by Lemma 3.2.

Proof. By (3.2), $G(x) = G_0(x) = -\frac{a_3}{5}x^2(x-t)^2(x-x_0)$ at (ω_0, γ_0) . Thus for (ω, γ) near (ω_0, γ_0) ,

$$G(x) = -\frac{1}{5}x^2(x-t)^2(x-x_0) + \frac{\omega - \omega_0}{2}x^2 + \frac{\gamma - \gamma_0}{2}x^4.$$

In both F*D and D*D cases, $a_3 = -1$ and $x_0 < 0$. The graph of G_0 is nonnegative for $0 < x < \infty$ and its only positive zero is $x = t$. The zero near t persists when $\omega < \omega_0$ and $\gamma < \gamma_0$, and converges to t as $\omega \rightarrow \omega_0^-$ and $\gamma \rightarrow \gamma_0^-$. The zero disappears when $\omega > \omega_0$ and $\gamma > \gamma_0$.

In the F*F case, $a_3 = 1$ and $x_0 \geq t$. For the non-endpoint case $t < x_0$, the graph of G_0 is nonnegative for $0 < x < x_0$ and it touches the x -axis at $x = t$ (see Figure 5). The zero near t persists when $\omega < \omega_0$ and $\gamma < \gamma_0$, and converges to t as $\omega \rightarrow \omega_0^-$ and $\gamma \rightarrow \gamma_0^-$. The zero near t disappears when $\omega > \omega_0$ and $\gamma > \gamma_0$, and the first positive zero jumps to near x_0 and converges to x_0 as $\omega \rightarrow \omega_0^+$ and $\gamma \rightarrow \gamma_0^+$. In the end point case $t = x_0$, the zero persists under any perturbation and converges to t in the limits. \square

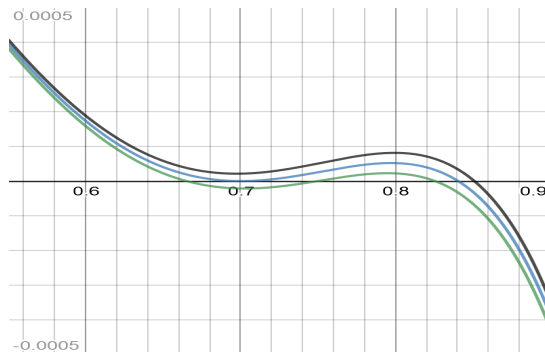


Figure 5: Perturbations of $G_0(x)$ with double zero $t = 0.7$, zero $x_0 = 0.8405$, FDF case.

3.4 Solutions inside the standing wave homoclinic orbit

In this Subsection we consider those $(\omega, \gamma) \in \mathbb{R}_+ \times \mathbb{R}$ such that (E1) and (E2) holds, the first positive zero ϕ_0 of G exists and is not a double zero. We want to study solutions of the planar system (2.5) that lie inside the homoclinic orbit passing $(\phi_0, 0)$ on the phase plane.

The following lemma implies that, in most cases, inside the homoclinic orbit passing $(\phi_0, 0)$ on the phase plane, there is only one fixed point $(x_1, 0)$, and any other solution is a periodic orbit around the fixed point. This is the familiar picture for a single power nonlinearity. However, there are exceptions in the FDF case $a_1 = a_3 = 1$ with $\gamma > \sqrt{3}$.

Lemma 3.6. *Fix $\omega > 0$ and $\gamma \in \mathbb{R}$. If the first positive zero ϕ_0 of G exists and $g(\phi_0) < 0$, there is a unique $x_1 \in (0, \phi_0)$ such that $g(x_1) = 0$ in the F*D, D*F and D*D cases. It is also true in the F*F case if $-\infty < \gamma \leq \sqrt{3}$.*

Proof. A positive zero of $g(x)$ is also a positive zero of

$$h(x) = \frac{g(x)}{x} = \omega - a_1x + \gamma x^2 - a_3x^3.$$

Note $h(0) > 0 > h(\phi_0)$ and hence h has a zero x_1 in $(0, \phi_0)$. If h has more than one zero in $(0, \phi_0)$, then it has 3 zeros

$$0 < x_1 \leq x_2 \leq x_3 < \phi_0, \quad x_1 < x_3.$$

Here we allow $x_1 = x_2$ or $x_2 = x_3$. Then $h(x)$ must have a local minimum x_- and a local maximum x_+ in $(0, \phi_0)$ with

$$0 < x_- < x_+ < \phi_0, \quad h(x_-) \leq 0 \leq h(x_+), \quad h(x_-) < h(x_+).$$

Thus $h'(x_-) = h'(x_+) = 0$ and x_{\pm} solve $3a_3x^2 - 2\gamma x + a_1 = 0$. Thus

$$x_{\pm} = \frac{1}{3a_3}(\gamma \pm \sqrt{\gamma^2 - 3a_1a_3}), \quad \gamma^2 > 3a_1a_3.$$

If $a_1 a_3 = -1$, then x_+ and x_- have opposite sign and is invalid.

We also have $h''(x_-) \geq 0 \geq h''(x_+)$. However, $h''(x) = 2\gamma - 6a_3x$, and we must have $a_3 = 1$. This excludes the D*D case.

The only remaining case is F*F $a_1 = a_3 = 1$. To avoid a contradiction to $x_{\pm} > 0$, we need $\gamma > \sqrt{3}$. \square

For the remaining FDF case $a_1 = a_3 = 1$ and $\gamma > \sqrt{3}$, there may be exceptions.

Example 3.7. Let $\omega = 0.1$ and $\gamma = 2.6$ in the FDF case. We have

$$\frac{g(x)}{x} = 0.1 - x + 2.6x^2 - x^3, \quad \frac{G(x)}{x^2} = 0.05 - \frac{x}{3} + \frac{2.6x^2}{4} - \frac{x^3}{5}.$$

Numerically, the first positive zero of G is $\phi_0 \approx 2.6585$. The positive zeros of g are approximately

$$x_1 = 0.1711, \quad x_2 = 0.2708, \quad x_3 = 2.1581.$$

See Figure 6. In this example, there are two homoclinic orbits on the phase plane starting from $(x_2, 0)$ and surrounding $(x_1, 0)$ and $(x_3, 0)$, respectively. Except these homoclinic orbits and fixed points, other solutions inside the standing wave orbit $(\phi, \dot{\phi})$ are periodic orbits. \square

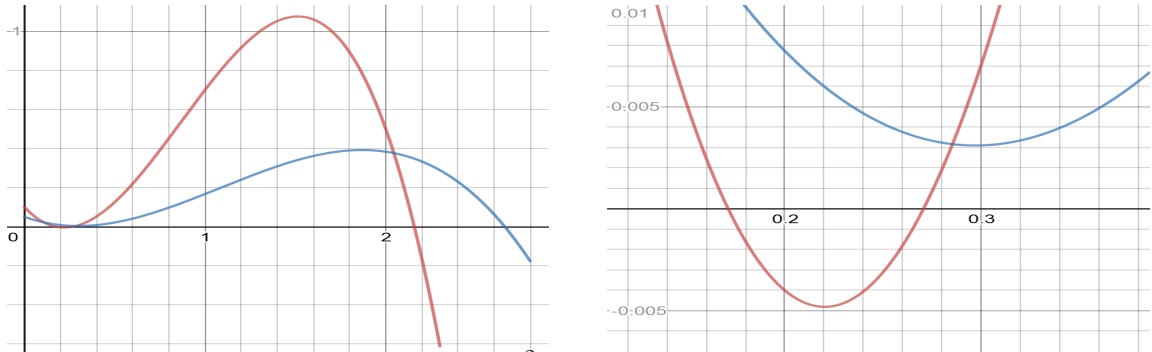


Figure 6: $g(x)/x$ (red) and $G(x)/x^2$ (blue) for $0 < x < 2.8$ and $0.12 < x < 0.38$

Example 3.8. A more systematic way is to consider

$$g(x) = -x(x - x_1)(x - x_2)(x - x_3), \quad x_1 = a, \quad x_2 = b, \quad x_3 = \frac{1 - ab}{a + b},$$

with parameters $a, b > 0$, $ab < 1$. It is of the form (1.6), i.e., $g(x) = \omega x - a_1 x^2 + \gamma x^3 - a_3 x^4$, with $a_1 = a_3 = 1$,

$$\omega = x_1 x_2 x_3 = \frac{ab(1 - ab)}{a + b}, \quad \gamma = x_1 + x_2 + x_3 = a + b + \frac{1 - ab}{a + b}.$$

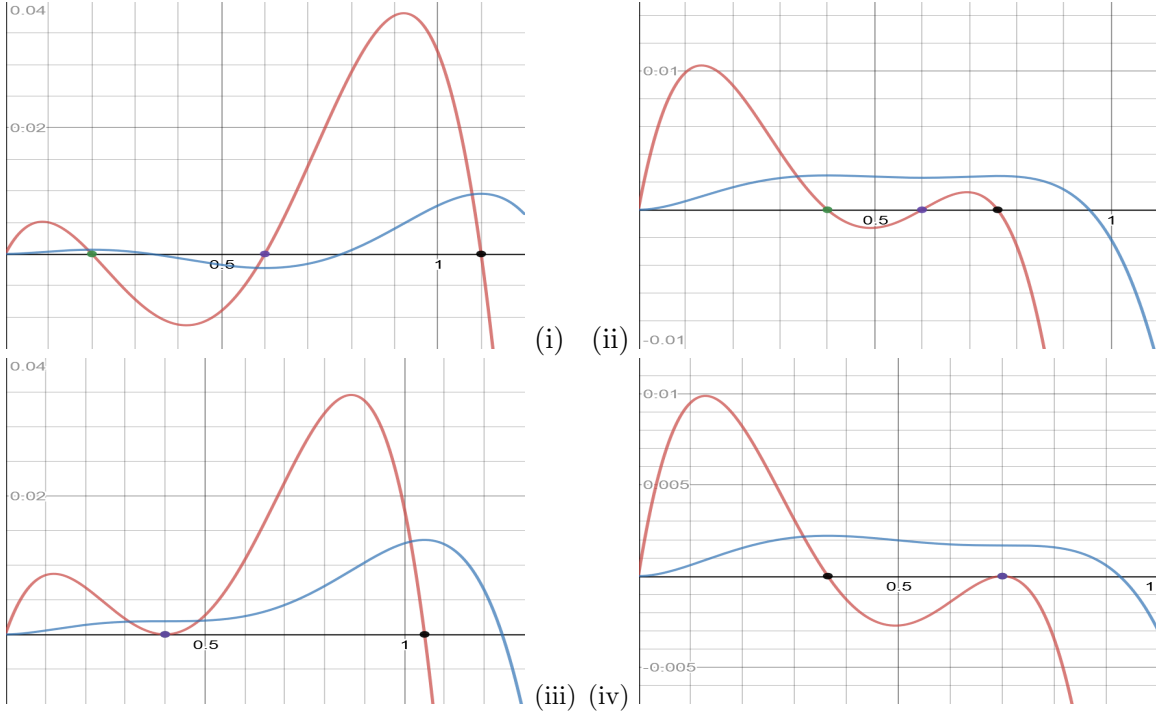


Figure 7: $g(x)$ (red) and $G(x)$ (blue) for (i) $(a, b) = (0.2, 0.6)$, (ii) $(a, b) = (0.4, 0.6)$, (iii) $a = b = 0.4$, (iv) $a = b = 0.7$

For some choices of a and b , g has only one zero in $(0, \phi_0)$. See Figure 7(i) for the case $(a, b) = (0.2, 0.6)$. For some other choices of a and b , g has three zeros in $(0, \phi_0)$, and we may have $x_1 = x_2$ or $x_2 = x_3$. See Figure 7(ii,iii,iv). We can decouple the double zero of g by decreasing ω slightly in (iii) and by increasing ω slightly in (iv). If we fix x_2 and let $x_1 \rightarrow x_2^-$, the homoclinic orbit around $(x_1, 0)$ and all orbits inside it collapse into $(x_2, 0)$. Similar phenomena happen if we fix x_2 and let $x_3 \rightarrow x_2^+$. \square

In general, the Jacobian matrix of the planar system $\dot{x} = y$, $\dot{y} = g(x)$ is

$$J = \begin{bmatrix} 0 & 1 \\ g'(x) & 0 \end{bmatrix}.$$

At a fixed point $(x_1, 0)$, the eigenvalues λ satisfy $\lambda^2 = g'(x_1)$. Thus, inside $(0, \phi_0)$,

1. if g has exactly one positive zero x_1 , then $g'(x_1) < 0$, and $\lambda \in i\mathbb{R}$, and $(x_1, 0)$ is a center. We expect periodic orbits around it.
2. If g has three distinct positive zeros $0 < x_1 < x_2 < x_3 < \phi_0$, then $g'(x_1) < 0$, $g'(x_2) > 0$, and $g'(x_3) < 0$. Thus $(x_1, 0)$ and $(x_3, 0)$ are centers, while $(x_2, 0)$ is a saddle.
3. In the degenerate case $x_1 = x_2$ or $x_2 = x_3$, the phase portrait can be derived as a limit of 3-distinct zero case.

4 Stability regions of parameters

In this section we study the stability of standing waves for those (ω, γ) in the existence region R_{ex} . In view of Proposition 2.2, we define the *stability functional*

$$J(\omega, \gamma) = \frac{d}{d\omega} \int \phi_{\omega, \gamma}^2(x) dx, \quad (\omega, \gamma) \in R_{\text{ex}}. \quad (4.1)$$

Equivalent integral formulas for J are given in (2.10)–(?). We now divide the existence region R_{ex} to 3 subregions:

1. $\Sigma_S = \{(\omega, \gamma) \in R_{\text{ex}} : J(\omega, \gamma) > 0\}$, stable region,
2. $\Sigma_U = \{(\omega, \gamma) \in R_{\text{ex}} : J(\omega, \gamma) < 0\}$, unstable region,
3. $\Gamma_{cr} = \{(\omega, \gamma) \in R_{\text{ex}} : J(\omega, \gamma) = 0\}$, where stability may change.

By Proposition 2.2, Σ_S corresponds to stable standing waves and Σ_U corresponds to unstable standing waves. The set Γ_{cr} is the boundary between Σ_S and Σ_U . It is called the *curve of stability change*, although in principle it may also contain points across which the standing waves do not change stability.

4.1 Limits of the stability functional J near the nonexistence curve

Proposition 4.1. *In all cases (F^*F , F^*D , D^*D) when Γ_{no} exists, for any $(\omega_0, \gamma_0) = (\omega(t), \gamma(t))$ given by (3.3) on Γ_{no} except the end point (ω_1, γ_1) in the FDF case, $J(\omega_0, \gamma_0)$ is undefined, and*

$$\lim_{\omega \rightarrow \omega_0-, \gamma \rightarrow \gamma_0-} J(\omega, \gamma) = +\infty. \quad (4.2)$$

*In the F^*F case, we also have*

$$\lim_{\omega \rightarrow \omega_0+, \gamma \rightarrow \gamma_0+} J(\omega, \gamma) = -\infty. \quad (4.3)$$

Note that the limits are taken through $(\omega, \gamma) \in R_{\text{ex}}$. Numerically, we also observe the above limits at (ω_1, γ_1) in the FDF case, and $\lim_{\omega \rightarrow \omega_1, \gamma \rightarrow \gamma_1} J(\omega, \gamma)$ does not exist. See next Subsection. We do not attempt to prove it as it is more technical due to the triple zero of G .

Proof. By (2.13),

$$J(\omega, \gamma) = \frac{-\sqrt{2}}{4g(\phi_0)} \int_0^{\phi_0} \frac{I(x, \omega, \gamma)}{\sqrt{G(x)}^3} dx, \quad (4.4)$$

where

$$I(x, \omega, \gamma) = 6\phi_0 x^2 G(x) + x^4 g(\phi_0) - \phi_0 x^3 g(x).$$

Note that ϕ_0 , g and G all depend on ω and γ . The integral is improper and I vanishes at both ends.

First consider the limit (4.2). By Lemma 3.5, $\phi_0(\omega_0-, \gamma_0-) = \phi_0(\omega_0, \gamma_0) = t$. The integrand of (4.4) is of order $O(1)$ for x near 0, and of order $O((\phi_0 - x)^{-1/2})$ for x near ϕ_0 . However, the former is uniformly integrable but the latter is not since $G = O((t - x)^2)$ for x near ϕ_0 in the limit. To study the integral for x near ϕ_0 , denote

$$I_1(x, \omega, \gamma) = \frac{I(x, \omega, \gamma)}{\phi_0 - x}.$$

It is continuous in all variables. In the limits $\omega \rightarrow \omega_0-$ and $\gamma \rightarrow \gamma_0-$, it is close to

$$I_1(x, \omega_0, \gamma_0) = \frac{6tx^2 G(x, \omega_0, \gamma_0) + 0 - tx^3 g(x, \omega_0, \gamma_0)}{t - x}.$$

Using (3.2) that $G(x) = -\frac{a_3}{5}x^2(x-t)^2(x-x_0)$ at (ω_0, γ_0) and $g = G'$, we have

$$\begin{aligned} I_1(x, \omega_0, \gamma_0) &= \frac{tx^3}{t-x} \frac{a_3}{5} (2x^2(x-t)(x-x_0) + O((x-t)^2)) \\ &= I_2(x) + O(x-t), \\ I_2 &= -\frac{2a_3}{5}tx^5(x-x_0), \end{aligned}$$

for x near t . In the F*F case, $a_3 > 0$ and $x_0 \geq t$. In the **D case, $a_3 < 0$ and $x_0 < 0$. In all cases, there is $0 < \delta \ll 1$ such that

$$\inf_{t-\delta < x < t} I_2(x) > 0; \quad \frac{1}{2}I_2(x) < I_1(x, \omega_0, \gamma_0) < 2I_2(x), \quad (t-\delta < x < t).$$

By continuity, for all $\omega < \omega_0$ and $\gamma < \gamma_0$ sufficiently close to (ω_0, γ_0) so that $\phi_0 < t$ is also close to t ,

$$\frac{1}{3}I_2(x) < I_1(x, \omega, \gamma) < 3I_2(x), \quad (t-\delta < x < t).$$

Decompose

$$J(\omega, \gamma) = \frac{-\sqrt{2}}{4g(\phi_0)} \left(\int_0^{t-\delta} + \int_{t-\delta}^{\phi_0} \right) \frac{(\phi_0 - x)I_1}{\sqrt{G}^3} dx = \frac{-\sqrt{2}}{4g(\phi_0)} (K_1(\omega, \gamma) + K_2(\omega, \gamma)).$$

$K_1(\omega, \gamma)$ is uniformly bounded in (ω, γ) while

$$K_2(\omega, \gamma) \geq \int_{t-\delta}^{\phi_0(\omega, \gamma)} \frac{(\phi_0 - x)I_2(x)}{3\sqrt{G(x)}^3} dx,$$

which converges to $+\infty$ as $\omega \rightarrow \omega_0-$ and $\gamma \rightarrow \gamma_0-$, noting that $G(x) = O((x-t)^2)$ and the integrand is of order $O((x-t)^{-2})$ in the limits. Since $g(\phi_0) < 0$, this shows (4.2).

In the F*F case and $\omega \rightarrow \omega_0+$ and $\gamma \rightarrow \gamma_0+$, we have $\phi_0(\omega+, \gamma+) = x_0$ by Lemma 3.5. The integrand are bounded by $O(1)$ near 0 and by $(\phi_0 - x)^{-1/2}$ near ϕ_0 and uniformly integrable. However, the integrand is not uniformly integrable for x near t as G has a double zero at t in the limits: For x near t , we have

$$I(x, \omega, \gamma) \sim I(t, \omega_0+, \gamma_0+) = 6x_0t^2G(t) + t^4g(x_0) - x_0t^3g(t) = t^4g(x_0) < 0.$$

Above G and g are evaluated at (ω_0, γ_0) . Thus for $\delta > 0$ sufficiently small,

$$\int_{t-\delta}^{t+\delta} \frac{I(x, \omega, \phi)}{\sqrt{G(x)}^3} dx \leq \int_{t-\delta}^{t+\delta} \frac{t^4g(\phi_0)}{2\sqrt{G(x)}^3} dx \rightarrow -\infty$$

as $\omega \rightarrow \omega_0+$ and $\gamma \rightarrow \gamma_0+$. Thus the entire integral in (4.4) converges to $-\infty$. Since $g(\phi_0) < 0$, this shows (4.3). \square

4.2 Level sets of the stability functional J and stability regions

In this Subsection we present our numerical results for the level sets of $J(\omega, \gamma)$ on the ω - γ half plane, for F*F, F*D, D*F and D*D cases. See Figures 8-11.

4.2.1 Level sets for F*F case

By Theorem 3.4, R_{ex} is the entire ω - γ half plane except the non-existence curve Γ_{no} given by (3.6).

As shown in Figure 8, also see Figure 12 in §5.1, the curve of stability change Γ_{cr} , defined as the level set of $J = 0$, is a graph of the form $\gamma = \bar{\gamma}(\omega)$ defined for $\omega_1 < \omega < \infty$. It emanates from the end point $(\omega_1, \gamma_1) \approx (0.1656, 1.7889)$ of Γ_{no} , given by (3.9), and appears to have the same limiting slope given by (3.5),

$$\lim_{(\omega, \gamma) \in \Gamma_{\text{no}} \rightarrow (\omega_1, \gamma_1)} \frac{d\gamma}{d\omega} = \lim_{t \rightarrow \frac{\sqrt{5}}{3}} -\frac{2}{t^2} = -\frac{18}{5}.$$

The curve $\gamma = \bar{\gamma}(\omega)$ appears to be smooth, and is decreasing until a critical point (ω_2, γ_2) , whose numerical value is

$$(\omega_2, \gamma_2) \approx (0.5548, 1.5817). \quad (4.5)$$

See (5.10) of §5.2 for a more accurate approximation. The curve Γ_{cr} then becomes increasing for all $\omega \in (\omega_2, \infty)$. The value $\gamma_2 \approx 1.5817$ is the global minimum of the function $\gamma = \bar{\gamma}(\omega)$.

The union of $\Gamma_{\text{no}} \cup \Gamma_{\text{cr}}$ appears to be a smooth and convex curve. Note that the smoothness and convexity of Γ_{no} , except at (ω_1, γ_1) , follow from (3.5) and (3.6). That of Γ_{cr} is only numerically observed. For fixed $\omega \in (\omega_1, \infty)$, $J(\omega, \gamma)$ is defined and continuous for all $\gamma \in \mathbb{R}$. It is possible to show that $J(\omega, \gamma_-) > 0$ for some negative γ_- , $J(\omega, \gamma_+) < 0$ for some positive γ_+ , and hence $J(\omega, \gamma) = 0$ for some $\gamma \in (\gamma_-, \gamma_+)$ by the intermediate value theorem. However, it will require more work to show its uniqueness.

The stability functional $J(\omega, \gamma)$ has positive values below the union of $\Gamma_{\text{no}} \cup \Gamma_{\text{cr}}$, and has negative values above it. Thus the region below the union of $\Gamma_{\text{no}} \cup \Gamma_{\text{cr}}$ is the stable region Σ_S , and the region above it is the unstable region Σ_U .

For any fixed $c \neq 0$, the level curve $J = c$ is a connected curve. It also comes out from (ω_1, γ_1) , with the same limiting slope $-\frac{18}{5}$. It diverges away from Γ_{cr} as ω increases, with a negative slope.

When $c > 0$, the curve continues until it reaches to a specific ω , and turns back toward $\omega = 0$, first with a positive slope, and then gradually switching to a negative slope. The value of γ eventually goes to positive infinity, while $\omega \rightarrow 0_+$.

When $c < 0$, the curve continues and changes to a positive slope at some point, until it reaches to a specific ω , and turns back toward $\omega = 0$ with a negative slope. The value of γ eventually goes to positive infinity, while $\omega \rightarrow 0_+$.

In both cases $c > 0$ and $c < 0$, the level curve $J = c$ emits from (ω_1, γ_1) , changes slope sign twice, and eventually $(\omega, \gamma) \rightarrow (0_+, +\infty)$.

The picture agrees with Proposition 4.1 that, for any $(\omega_0, \gamma_0) \in \Gamma_{\text{no}} \setminus \{(\omega_1, \gamma_1)\}$, we have

$$\lim_{\omega \rightarrow \omega_0^-, \gamma \rightarrow \gamma_0^-} J(\omega, \gamma) = +\infty, \quad \lim_{\omega \rightarrow \omega_0^+, \gamma \rightarrow \gamma_0^+} J(\omega, \gamma) = -\infty.$$

Since all level curves turn toward γ -axis, it seems that the function $\omega \mapsto \sup_{\gamma \in \mathbb{R}} |J(\omega, \gamma)|$ is finite and decreasing in ω , with

$$\lim_{\omega \rightarrow \infty} \sup_{\gamma \in \mathbb{R}} |J(\omega, \gamma)| = 0.$$

For stability, it follows from Proposition 2.2 that, for all (ω, γ) above $\gamma = \bar{\gamma}(\omega)$, the solution $\phi(x)e^{i\omega t}$ is orbital unstable. For all (ω, γ) below $\gamma = \bar{\gamma}(\omega)$, the solution $\phi(x)e^{i\omega t}$ is orbital stable. In particular, if $-\infty < \gamma < \gamma_2$, the solution $\phi(x)e^{i\omega t}$ is orbital stable for all $\omega > 0$.

For the borderline standing waves $\phi_{\omega, \bar{\gamma}(\omega)} e^{i\omega t}$, $\omega_1 < \omega < \infty$, by Comech and Pelinovsky [8], (also see [7] for gKdV), we expect them to be unstable for all $\omega \neq \omega_2$. It would be interesting to investigate the stability of the standing wave $\phi_{\omega_2, \gamma_2} e^{i\omega_2 t}$, since at $\gamma = \gamma_2$, all standing waves $\phi_{\omega, \gamma_2} e^{i\omega t}$ should be stable if $\omega \neq \omega_2$. The assumptions in [8] for borderline standing waves likely fail for this degenerate case.

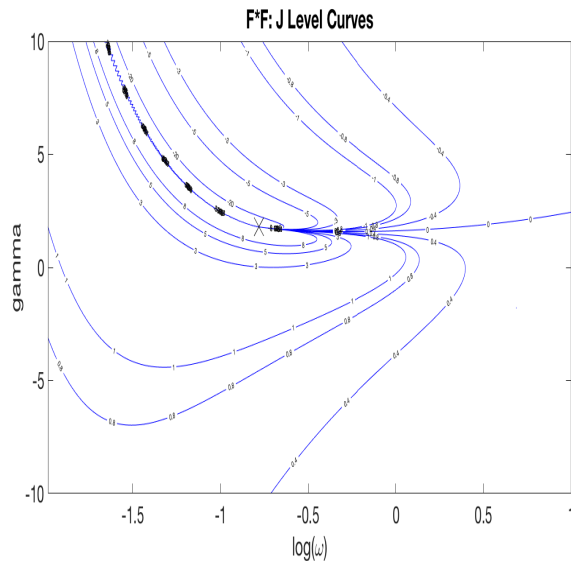


Figure 8: (i) F*F case

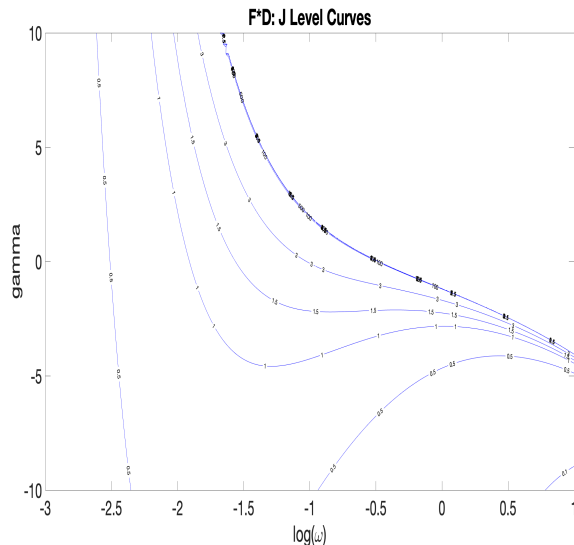


Figure 9: (ii) F*D case

4.2.2 Level sets for F*D case

By Theorem 3.4, R_{ex} is the region below the non-existence curve Γ_{no} given by (3.7). Note that R_{ex} and Γ_{no} are present in both FDD ($\gamma > 0$) and FFD ($\gamma < 0$) subcases.

As shown in Figure 9, J is positive in entire R_{ex} . Hence every standing wave is orbital stable by Proposition 2.2.

Agreeing with Proposition 4.1, the values of J converge to positive infinity as (ω, γ) converges to Γ_{no} .

4.2.3 Level sets for D*F case

By Theorem 3.4, R_{ex} is the entire ω - γ half plane.

As shown in Figure 10, the curve of stability change Γ_{cr} , defined as the level set of $J = 0$, is a graph of the form $\gamma = \bar{\gamma}(\omega)$ defined for all $0 < \omega < \infty$. The curve is increasing for all ω . It appears to have a finite limit as $\omega \rightarrow 0_+$. Numerically, the closest point in our computation is

$$(\omega, \gamma) = (0.001, -3.83459),$$

as we cannot start from $\omega = 0$. The values of J are positive below Γ_{cr} , and negative above Γ_{cr} . Thus the region below Γ_{cr} is the stable region Σ_S , and the region above Γ_{cr} is the unstable region Σ_U .

We expect the borderline standing waves $\phi_{\omega, \bar{\gamma}(\omega)} e^{i\omega t}$, $0 < \omega < \infty$ to be unstable by Comech and Pelinovsky [8], if we could analyze $\gamma = \bar{\gamma}(\omega)$ analytically.

The value of J increases in magnitude as (ω, γ) diverges from the curve of stability change Γ_{cr} . Globally, we also observe

$$\lim_{\omega \rightarrow \infty} \sup_{\gamma \in \mathbb{R}} |J(\omega, \gamma)| = 0.$$

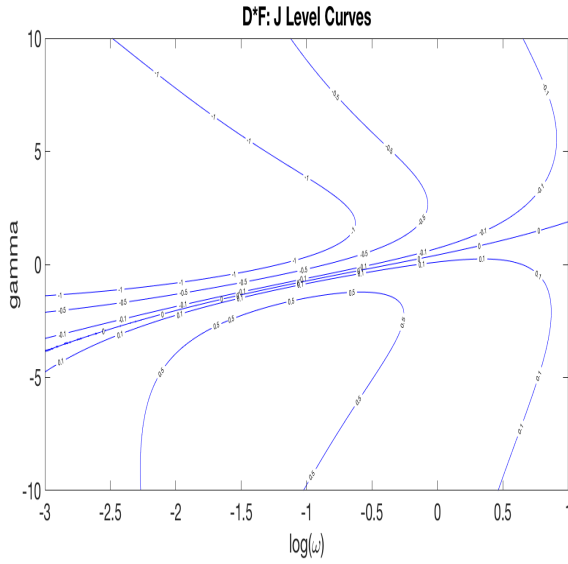


Figure 10: (iii) D*F case

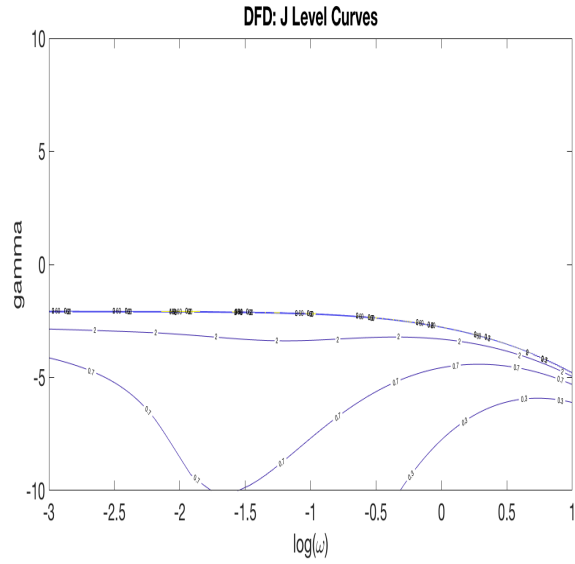


Figure 11: (iv) D*D case

4.2.4 Level sets for D*D case

By Theorem 3.4, R_{ex} is the region below the non-existence curve Γ_{no} given by (3.8). Note that R_{ex} and Γ_{no} are present only in the DFD ($\gamma < 0$) subcase. Indeed, since $(\omega, \gamma) \rightarrow (0, -\frac{8\sqrt{15}}{15})$ as $t \rightarrow \sqrt{\frac{5}{3}}+$, we have

$$\gamma < -\frac{8\sqrt{15}}{15} \approx -2.06559.$$

As shown in Figure 11, J is positive in entire R_{ex} . Hence every standing wave is orbital stable by Proposition 2.2.

Agreeing with Proposition 4.1, the values of J converge to positive infinity as (ω, γ) converges to Γ_{no} .

5 Numerics

In this section we discuss our numerical methods and observations.

In Subsection 5.1, we describe the computations of the level curves of the stability functional $J(\omega, \gamma)$ and the stability regions for the four cases: F*F, F*D, D*F, and D*D in the right half ω - γ plane. The numerical results of all four cases agree with Theorem 3.4 and Proposition 4.1.

In Subsection 5.2, we describe the computation of the curve of stability change Γ_{cr} and its minimal point (ω_2, γ_2) in the F*F case. Our first method is based in successive zoom-in windows. Our second method is based on the `fsolve` command of MATLAB. Our most accurate approximation of (ω_2, γ_2) is in (5.10).

In Subsection 5.3, we describe the 3 methods that we use for computing the standing wave $\phi_{\omega, \gamma}$. Our computed $\phi_{\omega, \gamma}$ agrees in the behaviour of the standing wave given by the planar dynamics.

5.1 Level curves and stability regions

In this Subsection we describe how we obtain the level curves and stability regions numerically. In MATLAB, we implement the existence condition (2.9) into three “if” statements. The pairs (ω, γ) passing through all “if” statements are then categorized into stable, unstable, or boundary points by the value of $J(\omega, \gamma)$. We use (2.12), the formula for $d''(\omega)$, to numerically compute J in MATLAB. The figures of the stability regions for all 4 cases are presented in Section 4.2. Figure 12 is an additional plot of the level curves of J in the F*F case.

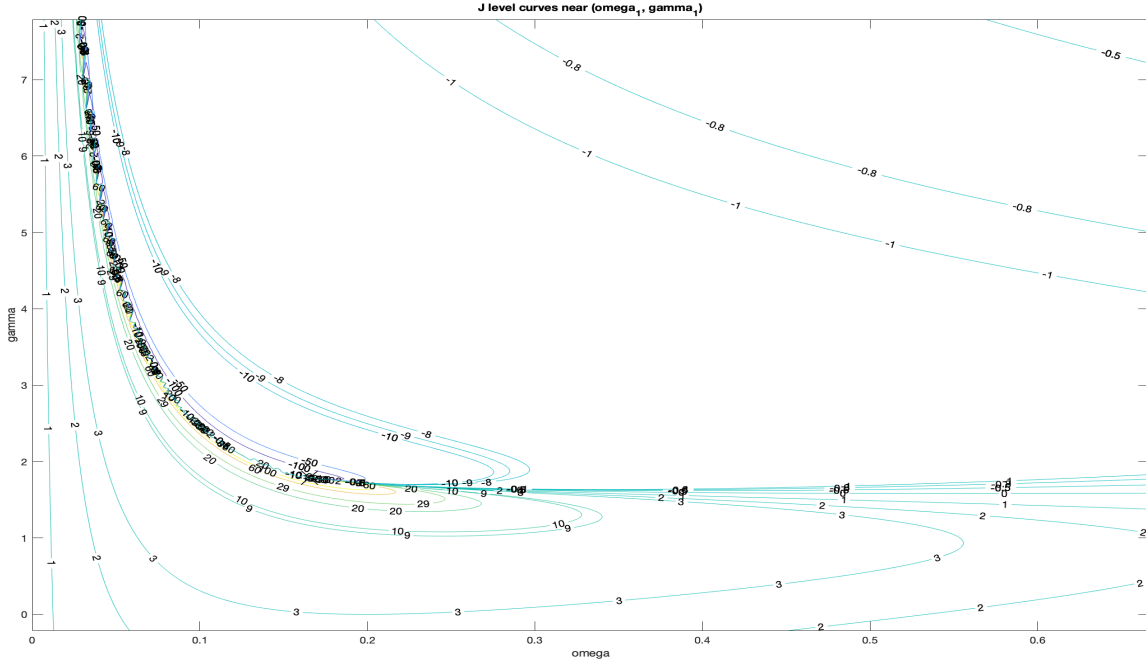


Figure 12: Level curves of J near (ω_1, γ_1) , F*F case.

The level curves of J are computed using MATLAB’s `contour` function, and the mesh sizes for all cases are described below:

For F*F case: For Figure 8:

$(\omega, \gamma) \in [0.001, 0.0104] \times [-10, 10]$: 900×900 mesh points.

$(\omega, \gamma) \in [0.0104, 0.603] \times [0, 10]$: 900×900 mesh points, containing (ω_1, γ_1) and (ω_2, γ_2)

$(\omega, \gamma) \in [0.0104, 0.603] \times [-10, 0]$: 900×900 mesh points.

$(\omega, \gamma) \in [0.603, 5] \times [-10, 10]$: 791×900 mesh points.

$(\omega, \gamma) \in [5, 10] \times [0, 10]$: 200×200 mesh points.

For Figure 12:

$(\omega, \gamma) \in [0.001, 0.603] \times [0, 10]$: 500×500 mesh points.

For F*D case: (Figures 9)

$(\omega, \gamma) \in [0.001, 0.01] \times [-10, 10]$: 450×900 mesh points.

$(\omega, \gamma) \in [0.01, 0.0243] \times [0, 10]$: 14×900 mesh points.

$(\omega, \gamma) \in [0.0243, 0.01102] \times [0, 10]$: 900×900 mesh points.

$(\omega, \gamma) \in [0.01102, 1] \times [0, 10]$: 807×900 mesh points.

$(\omega, \gamma) \in [0.01, 1] \times [-10, 0]$: 900×900 mesh points.

$(\omega, \gamma) \in [1, 5] \times [0, 10]$: 900×450 mesh points.

$(\omega, \gamma) \in [1, 10] \times [-10, 0]$: 900×900 mesh points.

$(\omega, \gamma) \in [5, 10] \times [0, 10]$: 200×100 mesh points.

For D*F case: (Figures 10)

$(\omega, \gamma) \in [0.001, 0.025] \times [-10, 10]$: 900×900 mesh points.

$(\omega, \gamma) \in [0.025, 5] \times [-10, 10]$: 896×900 mesh points.

$(\omega, \gamma) \in [5, 10] \times [-10, 10]$: 200×200 mesh points.

For DFD case: (Figures 11)

$(\omega, \gamma) \in [0.001, 5] \times [-10, 10]$: 900×900 mesh points.

$(\omega, \gamma) \in [5, 10] \times [-10, 10]$: 200×200 mesh points.

When we used mesh points less than numbers stated above, the results were some non continuous level sets and zigzag curves, especially near Γ_{no} . However, using the refined mesh sizes, we get smooth looking connected level sets.

5.2 The curve of stability change Γ_{cr} and its minimal point (ω_2, γ_2)

Recall Subsection 4.2.1 that, in the F*F case, the curve of stability change Γ_{cr} is numerically observed to be a graph $\gamma = \bar{\gamma}(\omega)$, $\omega_1 < \omega < \infty$, and its minimal γ -value occurs at a critical point (ω_2, γ_2) . We have

$$(\omega_1, \gamma_1) = \left(\frac{2\sqrt{5}}{27}, \frac{4\sqrt{5}}{5} \right) \approx (0.1656, 1.7889), \quad (\omega_2, \gamma_2) \approx (0.5548, 1.5817).$$

In this Subsection we describe how we get more accurate approximations of Γ_{cr} and (ω_2, γ_2) . Note that Γ_{cr} is only numerically observed without an analytic formula, and we have not proved its regularity, nor the existence of a unique minimum γ_2 of $\bar{\gamma}(\omega)$.

For our computation, we use the MATLAB default precision of 16 decimal digits.

Method 1. In our first method, we improve our approximations by computation in a sequence of shrinking windows in the ω - γ parameter domain. See Table 1.

window	ω range	γ range	mesh	$d\omega$	$d\gamma$	$\frac{d\omega}{d\gamma}$
W_1	$[\omega_1 + 10^{-4}, 1.6656]$	$[1.55, 1.8]$	300×1000	0.005	$2.5e-4$	20
W'_1	$[0.4, 0.7]$	$[1.57, 1.6]$	60×120	0.005	$2.5e-4$	20
W_2	$[0.5, 0.6]$	$[1.57, 1.59]$	200×800	$5e-4$	$2.5e-5$	20
W'_2	$[0.545, 0.565]$	$[1.5816, 1.5818]$	40×8	$5e-4$	$2.5e-5$	20
W_3	$[0.55, 0.56]$	$[1.58168, 1.58172]$	400×160	$2.5e-5$	$2.5e-7$	100
W'_3	$[0.55, 0.56]$	$[1.581704, 1.581714]$	400×40	$2.5e-5$	$2.5e-7$	100

Table 1: Windows of computation. $2.5e-5$ means $2.5 \cdot 10^{-5}$.

5.2.1 Window W_1

We start with the largest window

$$W_1 = [\omega_1 + 0.0001, 1.6656] \times [1.55, 1.8], \quad \text{mesh size: } 300 \times 1000.$$

The choice of W_1 is based on the computation results for Figures 8 and 12. Since $\omega_1 \approx 0.1656$,

$$d\omega \approx 0.005, \quad d\gamma = 0.00025, \quad \frac{d\omega}{d\gamma} = 20.$$

The ratio $d\omega/d\gamma = 20$ is chosen larger than 1 in anticipation of a flat slope of $\gamma = \bar{\gamma}(\omega)$ around $\omega = \omega_2$.

For each mesh point (ω_k, γ_l) we compute $J(\omega_k, \gamma_l)$ using (2.12).

In view of Figures 8 and 12, we anticipate that $J(\omega_k, \gamma_l)$ is decreasing in l at most points, except those close to (ω_1, γ_1) where some level curves of J turn around. This is reinforced by Figure 13 on the level curves of J in W_1 . One observes that the portion of the level curve $J = c$ after turn around does not intersect W_1 if $|c| < 20$. Hence $J(\omega_k, \gamma_l)$ is decreasing in l in W_1 as long as $|J(\omega_k, \gamma_l)| < 20$ (which is always the case for $\omega \geq 0.4$).

Thus, for each ω_k we define $\bar{\gamma}(\omega_k) = \gamma_l$ where γ_l is the smallest such that

$$J(\omega_k, \gamma_l) \geq 0 > J(\omega_k, \gamma_{l+1}). \quad (5.1)$$

This gives us a discrete curve $(\omega_k, \bar{\gamma}(\omega_k))_k$, shown as the dotted curve in Figure 14.

We then define the approximate γ_2 as

$$\gamma_2^* = \min_k \{\bar{\gamma}(\omega_k)\}, \quad (5.2)$$

and the ω -interval that attains γ_2^*

$$[\omega_{\min}^*, \omega_{\max}^*] = \{\omega_k : \bar{\gamma}(\omega_k) = \gamma_2^*\}. \quad (5.3)$$

We expect our true values of (ω_2, γ_2) satisfy

$$\bar{\gamma} \leq \gamma_2 \leq \bar{\gamma} + d\gamma, \quad \omega_{\min}^* - d\omega \leq \omega_2 \leq \omega_{\max}^* + d\omega.$$

We may take $\omega_2^* = \frac{1}{2}(\omega_{\min}^* + \omega_{\max}^*)$ as an approximation of ω_2 . We obtain

$$W_1 : \quad \gamma_2^* = 1.581531531531532, \quad \omega_2^* \in [0.541955066755841, 0.567036426872898]. \quad (5.4)$$

From Figure 14, we choose a subwindow W_1' that clearly contains the line segment $[\omega_{\min}^*, \omega_{\max}^*] \times \{\gamma_2^*\}$ and graph a zoomed picture in W_1' (using the previous computation result in W_1), see Figure 15. Using this finer picture we will choose our next window W_2 .

Method 2. Our second method is based on MATLAB's `fsolve` command, which solves a zero of a given function near a given initial point. It can be considered as a refinement of Method 1 since we use the results of Method 1 as our initial points. However, there are many other ways to choose initial points. For example, with an approximation curve $(\bar{\omega}_k, \bar{\gamma}_k)$ from a previous computation, we can insert N points between $(\bar{\omega}_k, \bar{\gamma}_k)$ and $(\bar{\omega}_{k+1}, \bar{\gamma}_{k+1})$ by linear interpolation for each k , and use the portion of this new curve that is near the minimal point as our new initial points.

Specifically, we use the 300 points

$$(\omega_k, \gamma(\omega_k)), \quad 1 \leq k \leq 300$$

obtained in Method 1 as the initial points, and use MATLAB's `fsolve` command with `levenberg-marquardt` algorithm option, to solve 300 zeros

$$(\bar{\omega}_k, \bar{\gamma}_k), \quad 1 \leq k \leq 300$$

of the stability functional $J(\omega, \gamma)$ that are close to $(\omega_k, \gamma(\omega_k))$. This parametric, discrete curve is shown as the solid curve in Figure 14. It is a finer approximation of the curve $\gamma = \bar{\gamma}(\omega)$ since the default precision of MATLAB when applying `fsolve` is 16 decimal digits, much less than our $d\gamma$. These points $(\bar{\omega}_k, \bar{\gamma}_k)$ are not mesh points, but it is fine.

We now define the approximate γ_2 and ω_2 as

$$\gamma_2^{**} = \min_k \{\bar{\gamma}_k\}, \quad \omega_2^{**} = \operatorname{argmin}_k \{\bar{\gamma}_k\}. \quad (5.5)$$

This time ω_2^{**} is attained at a single value of ω , not an interval as in Method 1. We obtain

$$W_1 : (\omega_2^{**}, \gamma_2^{**}) = (0.557003765501051, 1.58170639609768). \quad (5.6)$$

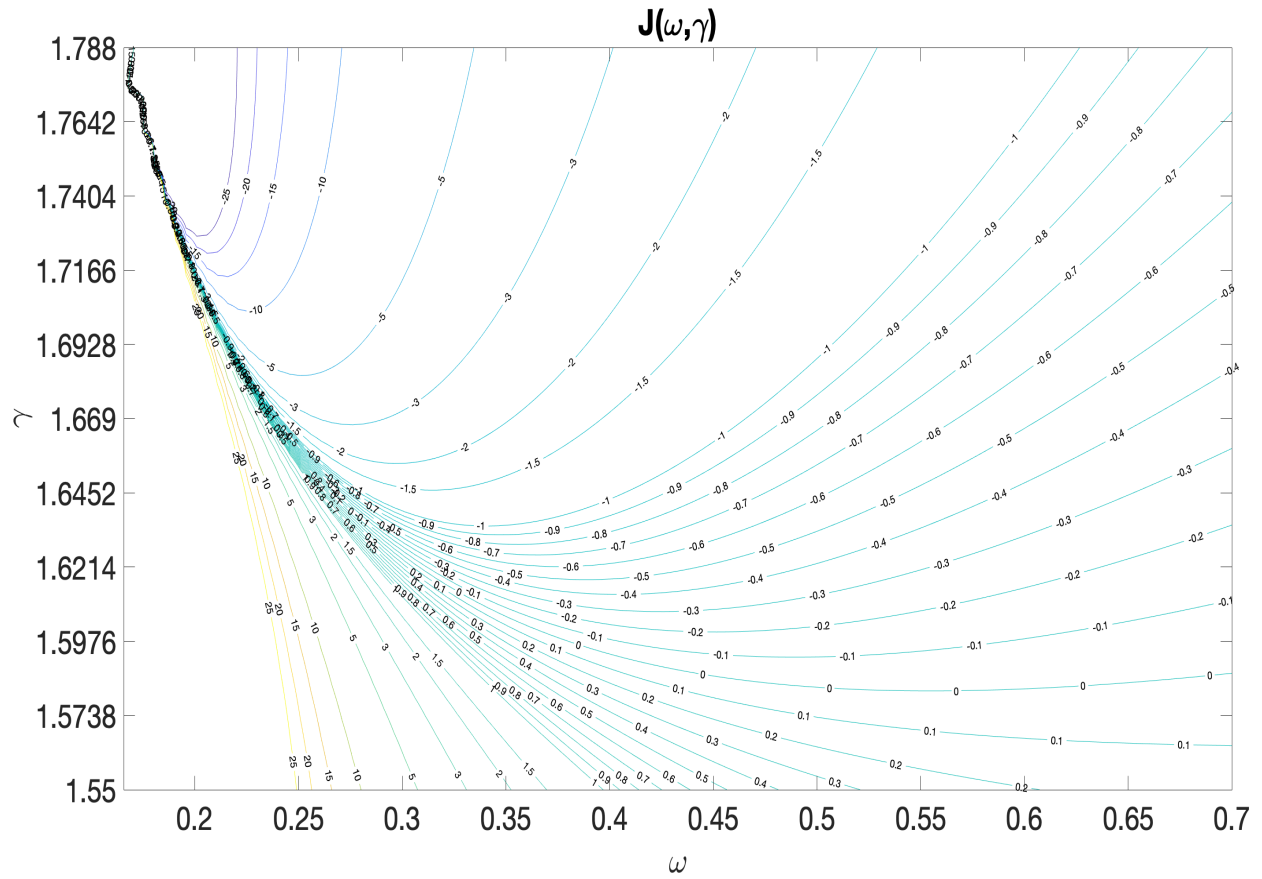


Figure 13: Level curves of J in the left half of window W_1 , F*F case.

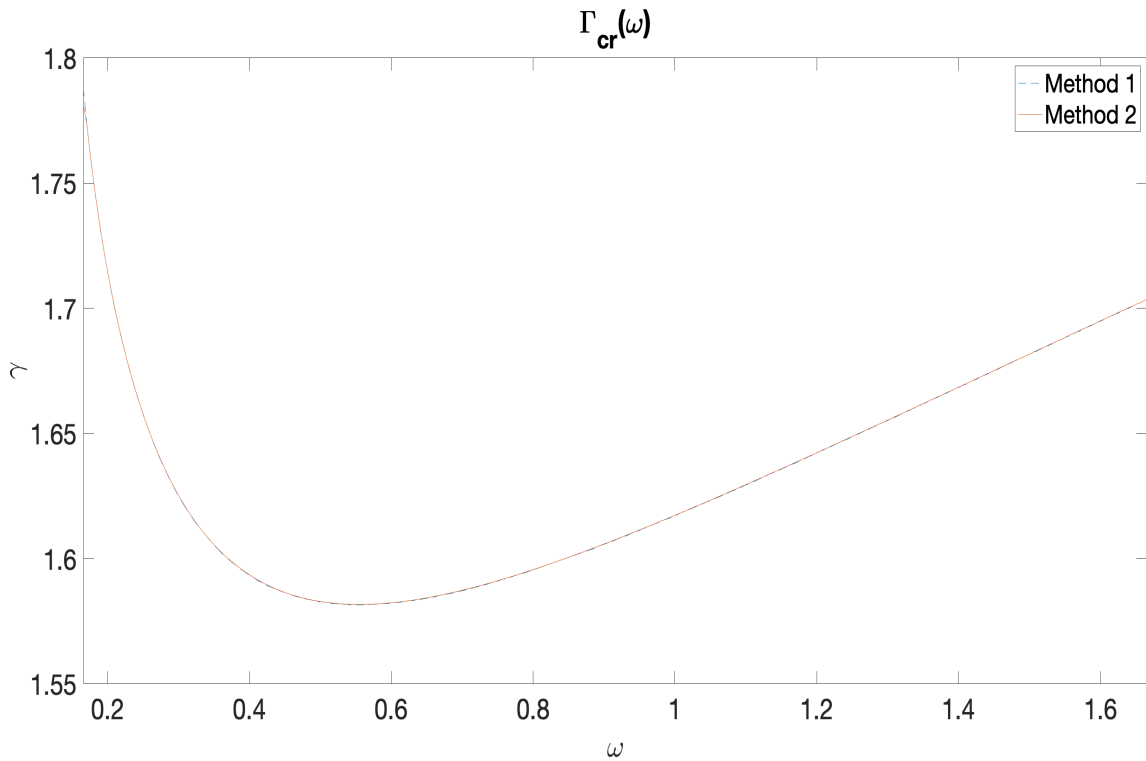


Figure 14: Γ_{cr} in W_1 .

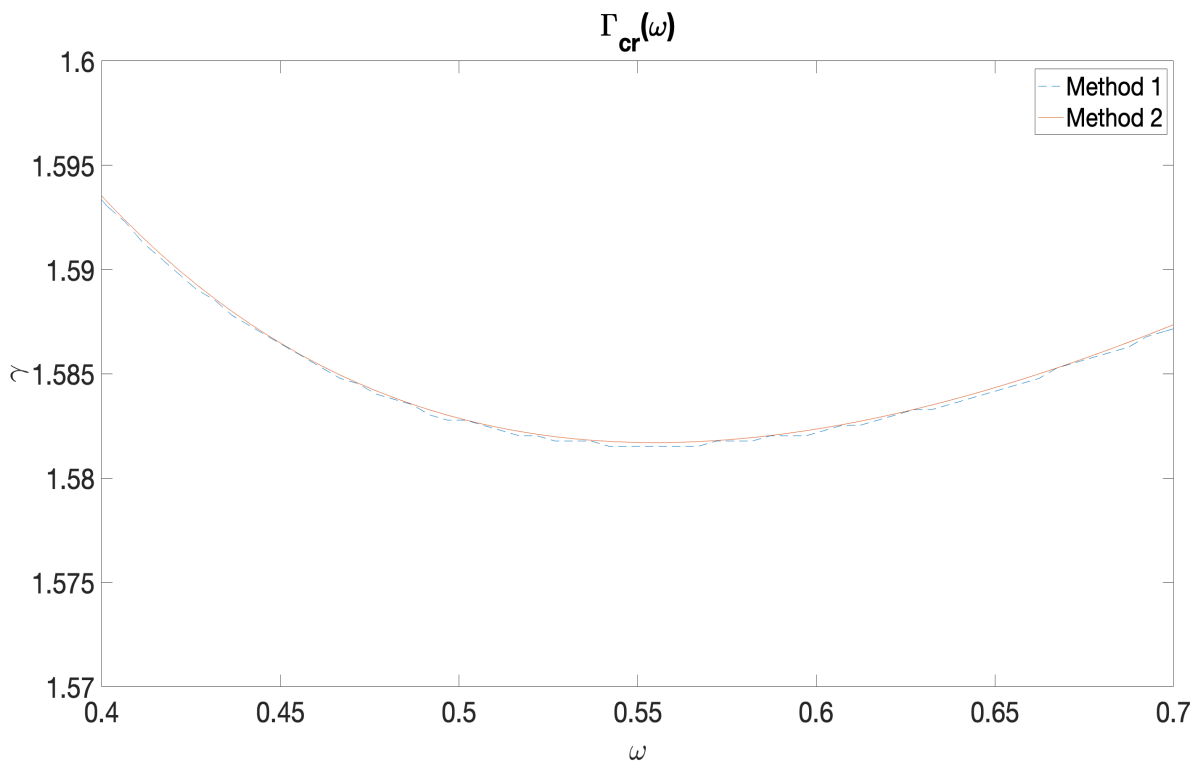


Figure 15: Γ_{cr} in W'_1

5.2.2 Window W_2

Based on Figure 15 on the curve Γ_{cr} in window W'_1 , we choose our second window

$$W_2 = [0.5, 0.6] \times [1.57, 1.59], \quad \text{mesh size: } 200 \times 800.$$

We do not increase the ratio $d\omega/d\gamma = 20$ since the mesh of W'_1 in Table 1 has more vertical points, which indicates that the ratio 20 is sufficient.

We repeat Methods 1 and 2 for window W_2 . Note that W_2 is away from (ω_1, γ_1) and $J(\omega_k, \gamma_l)$ is decreasing in l at *all* mesh points in W_2 . The approximation curves based on Methods 1 and 2 are presented in Figure 16. We also choose a subwindow $W'_2 = [0.545, 0.565] \times [1.5816, 1.5818]$, presented in Figure 17, for the choice of W_3 .

We obtain, by Method 1:

$$W_2 : \quad \gamma_2^* = 1.58168961201502, \quad \omega_2^* \in [0.549748743718593, 0.559798994974874], \quad (5.7)$$

and by Method 2:

$$W_2 : \quad (\omega_2^{**}, \gamma_2^{**}) = (0.554773875083001, 1.58170476081013). \quad (5.8)$$

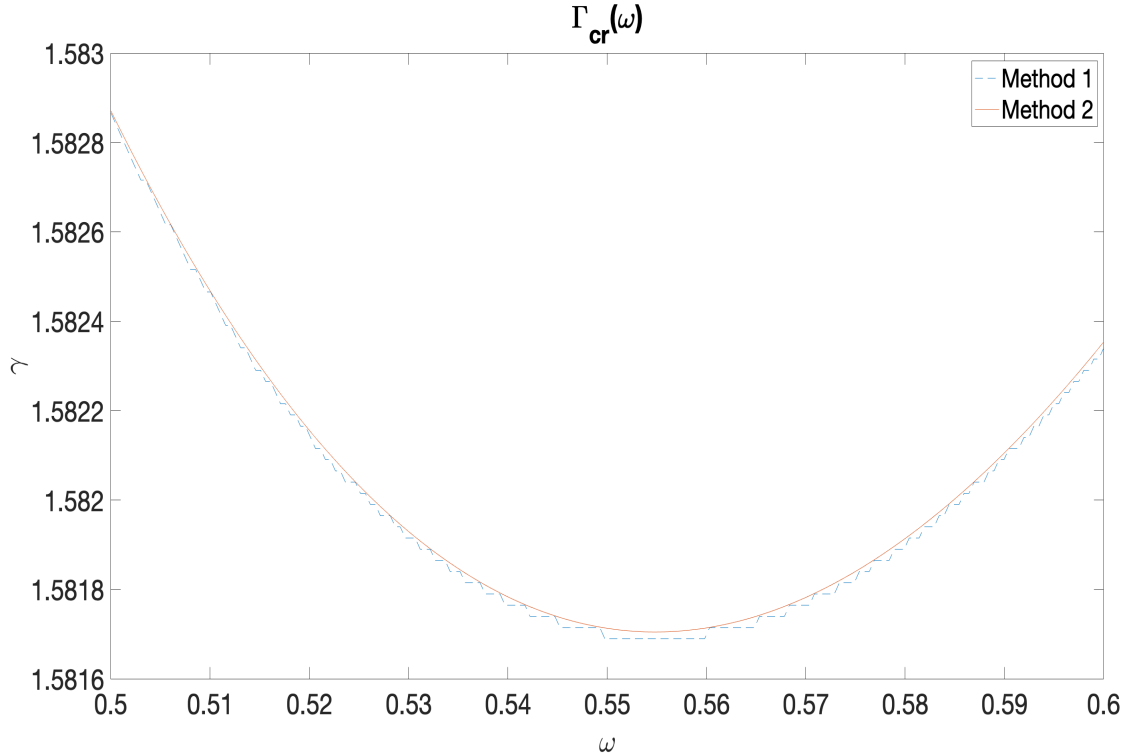


Figure 16: Γ_{cr} in W_2

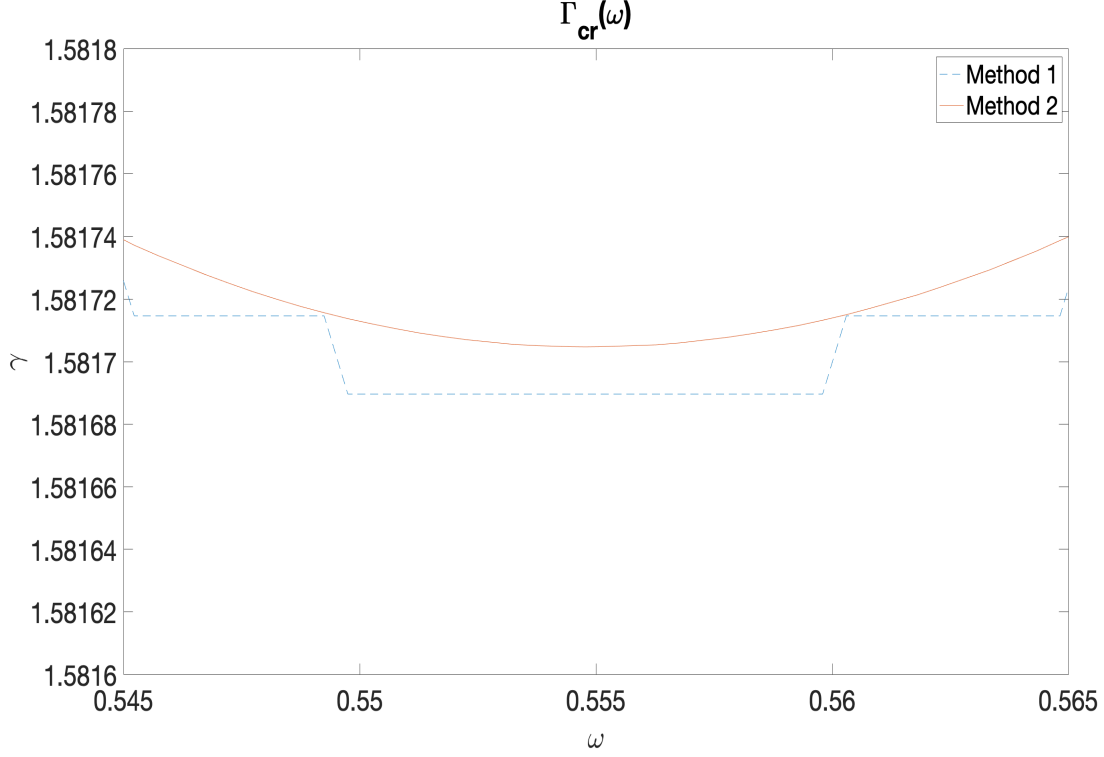


Figure 17: Γ_{cr} in W'_2

5.2.3 Window W_3

Based on Figure 17 on the curve Γ_{cr} in window W'_2 , we choose our third window

$$W_3 = [0.55, 0.56] \times [1.58168, 1.58172], \quad \text{mesh size: } 400 \times 160.$$

We increase the ratio $d\omega/d\gamma$ from 20 to 100 since the mesh of W'_2 in Table 1 has 5 times horizontal points than vertical points.

We repeat Methods 1 and 2 for window W_3 . The approximation curves based on Methods 1 and 2 are presented in Figure 18. We also choose a subwindow $W'_3 = [0.545, 0.565] \times [1.581704, 1.581714]$, presented in Figure 19, for a better local view.

We obtain, by Method 1:

$$W_3 : \quad \gamma_2^* = 1.58170465408805, \quad \omega_2^* \in [0.554185463659148, 0.55546365914787], \quad (5.9)$$

and by Method 2:

$$W_3 : \quad (\omega_2^{**}, \gamma_2^{**}) = (0.554837092755109, 1.58170475989899). \quad (5.10)$$

Eq. (5.10) is our best approximation of (ω_2, γ_2) . We collect $(\omega_2^{**}, \gamma_2^{**})$ in 3 windows in Table 2. Also included are $\Delta\omega_2^{**}$ and $\Delta\gamma_2^{**}$, the difference of the current values of $\omega_2^{**}, \gamma_2^{**}$ and their values in the previous window. The accuracy of γ_2^{**} is about 10^{-9} , but the accuracy of ω_2^{**} is about 10^{-4} , much larger. It is reasonable because the slope of $\bar{\gamma}(\omega)$ is close to zero near (ω_2, γ_2) .

window	ω_2^{**}	γ_2^{**}	$\Delta\omega_2^{**}$	$\Delta\gamma_2^{**}$
W_1	0.557003765501051	1.58170639609768	N/A	N/A
W_2	0.554773875083001	1.58170476081013	-2.22989041805e-3	-1.63528755e-6
W_3	0.554837092755109	1.58170475989899	6.3217672108e-5	-9.1114e-10

Table 2: $(\omega_2^{**}, \gamma_2^{**})$ in 3 windows

We could continue this zoom-in process and compute in smaller and smaller windows. However, three windows should be sufficient for illustration.

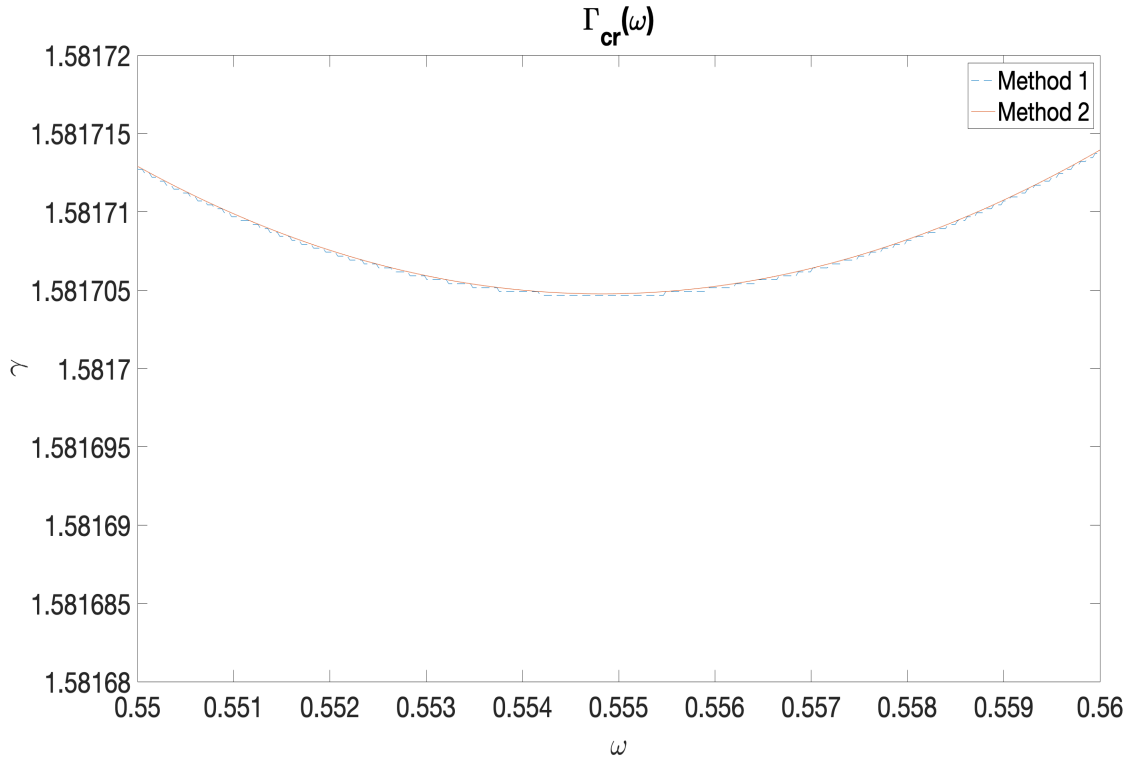


Figure 18: Γ_{cr} in W_3

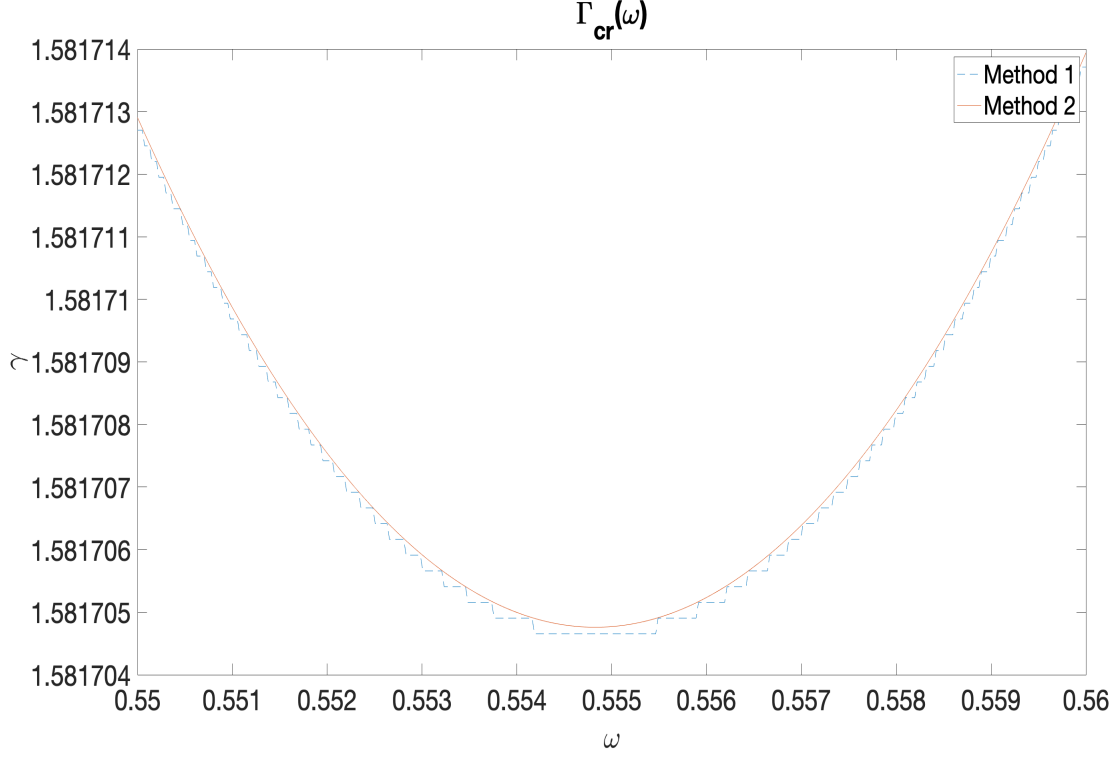


Figure 19: Γ_{cr} in W'_3

5.3 The standing waves

In this Subsection we describe how to compute the standing waves $\phi_{\omega,\gamma}$ numerically. For one dimensional NLS (1.1) considered in this paper, because we have formula (2.10) for the stability functional $J(\omega, \gamma) = d''(\omega)$, we do not need to compute $\phi_{\omega,\gamma}$ to determine the stability of $\phi_{\omega,\gamma}$. However, when we study the same NLS in a higher dimensional setting, formula (2.10) is not available. What we can do is to compute $\phi_{\omega,\gamma}$ and

$$N(\omega, \gamma) = d'(\omega) = \int_{\mathbb{R}^n} \phi_{\omega,\gamma}^2(x) dx,$$

and compare it with $N(\omega + d\omega, \gamma)$ to determine the sign of $d''(\omega)$. Thus it is still relevant to be able to compute the standing waves $\phi_{\omega,\gamma}$ numerically.

In the 1D setting, for given (ω, γ) , $\phi_{\omega,\gamma}(t)$ solves (1.6),

$$\phi'' = g(\phi) = \omega\phi - a_1|\phi|\phi + \gamma|\phi|^2\phi - a_3|\phi|^3\phi, \quad (5.11)$$

with $a_1, a_3 = \pm 1$, $\phi(t) > 0$ and $\lim_{t \rightarrow \pm\infty} \phi(t) = 0$. We will focus on the FDF case, $a_1 = a_3 = 1$ and $\omega, \gamma > 0$. We can translate t so that $\phi(0) = \max \phi$, and we have the boundary conditions

$$\phi(0) = \phi_0, \quad \phi'(0) = 0, \quad \lim_{t \rightarrow \infty} \phi(t) = 0, \quad (5.12)$$

where $\phi_0 = \max \phi = \phi_0(\omega, \gamma)$ is the first positive zero of the potential function $G(t)$ given in (3.1) or, equivalently, the first positive zero of

$$\omega = \frac{2}{5}x^3 - \frac{\gamma}{2}x^2 + \frac{2}{3}x. \quad (5.13)$$

We have tried the following three numerical methods and their combinations to compute $\phi_{\omega,\gamma}(t)$ with MATLAB. We usually start with the time interval $0 \leq t \leq 50$, and shift to smaller time intervals if necessary, e.g., when we take smaller dt and need more computation power.

Recall that there is no solution for $(\omega, \gamma) \in \Gamma_{\text{no}}$. For $(\omega, \gamma) \notin \Gamma_{\text{no}}$, the computation results usually look fine. However, smaller dt is required if (ω, γ) is close to Γ_{no} . It is because that, in this case, the solution of the planar dynamics (2.5) with $(x(0), y(0)) = (\phi_0, 0)$ spends a long time in the neighborhood of $(\phi_0, 0)$ where its velocity $(y, g(x))$ is extremely small. After it leaves the neighborhood, it moves rapidly toward the origin. Hence it is a stiff computational problem when (ω, γ) is close to Γ_{no} .

5.3.1 Shooting method

In this method, we compute solutions $\phi(t) = \phi_{\omega,\gamma}(t)$ of the problem (5.11) with initial conditions

$$\phi(0) = \phi_0, \quad \phi'(0) = 0, \quad (5.14)$$

for $t \in [0, 50]$ with mesh size $\Delta t = 0.00001$, using MATLAB command `ode45`.

The Shooting method alone usually first gives a reasonable decaying $\phi(t)$ for some time. However, it then bounces back and starts oscillating, becoming a periodic solution in the long time. Although theoretically the solution should converge to the origin, corresponding to a homoclinic orbit passing $(\phi_0, 0)$ on the phase plane, numerical errors likely perturb the solution to a nearby periodic orbit. (It looks periodic, but most likely is not, again due to numerical errors.) Since the oscillation is due to numerical error, it should be truncated. In Figure 20 we present solutions for $\gamma = 1.8$ and several ω .

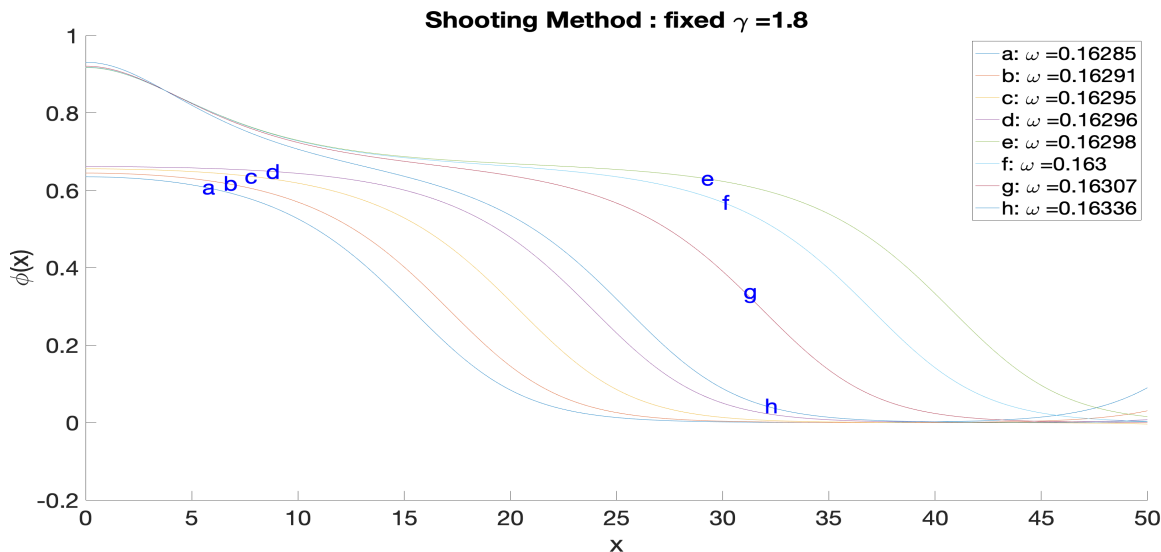


Figure 20: Method 1 for $\gamma = 1.8$ and several ω 's.

Recall that Γ_{no} ends at $(\omega_1, \gamma_1) \approx (0.1656, 1.7889)$ and $\gamma = 1.8$ is slightly larger than γ_1 . The values of ω in Figure 20 are close to $\omega_0 = \frac{22}{135} \approx 0.162963$, which is such that $(\omega_0, 1.8) \in \Gamma_{\text{no}}$. The closer ω to ω_0 , the longer the solution stay near its peak ϕ_0 . As a result, the supports of the solutions in Figure 20 are between 25 and 50, larger than those to be found for $\gamma = 1.7$ in Figure 22.

Recall that $\phi(0) = \phi_0$ is the first positive zero of (5.13) and $(\omega, \gamma) \in \Gamma_{\text{no}}$ if ϕ_0 is a double zero of (5.13). When $\gamma = 1.8$, $\phi_0 = 2/3$ is a double zero when $\omega = \omega_0 = \frac{22}{135}$. In this case,

(5.13) can be factorized as

$$\frac{2}{5}\left(x - \frac{2}{3}\right)^2\left(x - \frac{11}{12}\right) = 0,$$

and $\frac{11}{12}$ is the third zero. See Figure 21 for the graph of the right side of (5.13) when $\gamma = 1.8$. Thus when $\omega \rightarrow \omega_0^-$, ϕ_0 is increasing and converges to $\frac{2}{3}$. When $\omega \rightarrow \omega_0^+$, ϕ_0 is decreasing and converges to $\frac{11}{12}$. There is a jump from $\frac{2}{3}$ to $\frac{11}{12}$. This can be observed in Figure 20. In both intervals of ω , $(0, \omega_0)$ and (ω_0, ∞) , $\phi_0(\omega, 1.8)$ is an increasing function of ω .



Figure 21: Graph of the right side of (5.13) for the relation of ϕ_0 and ω when $\gamma = 1.8$.

Another difficulty of the Shooting method occurs for large ω and γ . For example, for $(\omega, \gamma) = (10, 5)$ and $dt = 0.001$, the computation stops at $t = 10.6355$ and we get the error message:

Warning: Failure at t=1.063551e+01. Unable to meet integration tolerances without reducing the step size below the smallest value allowed (2.842171e-14) at time t.

At $t = 10.6355$ the solution is small and hence has the same behavior as the solution of the linear ODE

$$\ddot{x} = \omega x$$

which has eigenvalues $\pm\sqrt{\omega}$. One may imagine that a larger ω corresponds to a larger positive eigenvalue and requires a smaller step size. If we fix $\gamma = 5$, the larger the value of ω , the smaller the stop time. See Table 3.

ω	5	10	15	20
stop time	1.330625e+01	1.063551e+01	8.375157e+00	7.429009e+00

Table 3: stop time of shooting method for $\gamma = 5$ and various large ω

A reasonable approximation is to keep the solution for $0 < t < T_1$, where T_1 is either the first positive time that the solution has zero derivative, the time that the solution goes below zero, or the time an error occurs. One then replaces the solution by zero for $t > T_1$. We call it the *shooting-cropping solution*.

5.3.2 Picard iteration method

In this method we refine our approximation solutions using the Picard iteration, starting from a good initial approximation. For the initial approximation we use the shooting-cropping solution from our first method.

We now describe the Picard iteration. For the ODE $\phi'' = g(\phi)$ — given in (5.11), suppose that we have a good initial guess u_0 . The difference $v = \phi - u_0$ satisfies

$$Lv = F(v) = F_0 + N(v), \tag{5.15}$$

where

$$Lv = v'' - g'(u_0)v, \\ F_0 = g(u_0) - u_0'', \quad N(v) = g(u_0 + v) - g(u_0) - g'(u_0)v.$$

The source term F_0 is independent of v and reasonably small if u_0 is a good guess. The term $N(v)$ is nonlinear in v and independent of ω .

Consider the finite difference discretization of the linear problem

$$Lv = F, \quad \text{in } (0, 50); \quad v(0) = v(50) = 0. \quad (5.16)$$

As $\phi = u_0 + v$, the boundary condition for ϕ ,

$$\phi(0) = \phi_0, \quad \phi(50) = 0, \quad (5.17)$$

is satisfied if u_0 also satisfies (5.17). Unlike $L_0 = v'' - \omega v$, problem (5.16) may not be invertible as L may have a kernel, $L\psi = 0$ for some $\psi \neq 0$. However, this is non-generic, and L should have no kernel if we simply perturb u_0 or the step-size slightly. Thus for most u_0 , (5.16) should correspond to an invertible vector equation in the finite difference method. Let $v = G(F)$ be the solution operator of the corresponding vector equation of (5.16) in the finite difference method. We can solve the solution v of (5.16) with $F = F(v)$ by Picard iteration

$$v^{(0)} = 0, \quad v^{(k+1)} = G(F(v^{(k)})), \quad k \geq 0. \quad (5.18)$$

A revised scheme is

$$v^{(1)} = G(F_0), \quad v^{(k+1)} = v^{(1)} + G(N(v^{(k)})), \quad k \in \mathbb{N}, \quad (5.19)$$

It seems more efficient as we only compute $v^{(1)}$ once.

Using this method, with dt as coarse as $dt = 0.1$, we already obtain reasonably monotonic decaying solutions which agree with the solutions obtained using $dt = 0.01$, and solutions obtained using Method 3. See Figure 22 for graphs by Method 2 for fixed $\gamma = 1.7$ and several ω . Note that $1.7 < \gamma_1 \approx 1.7889$. Hence $(\omega, 1.7) \notin \Gamma_{\text{no}}$ for all ω .

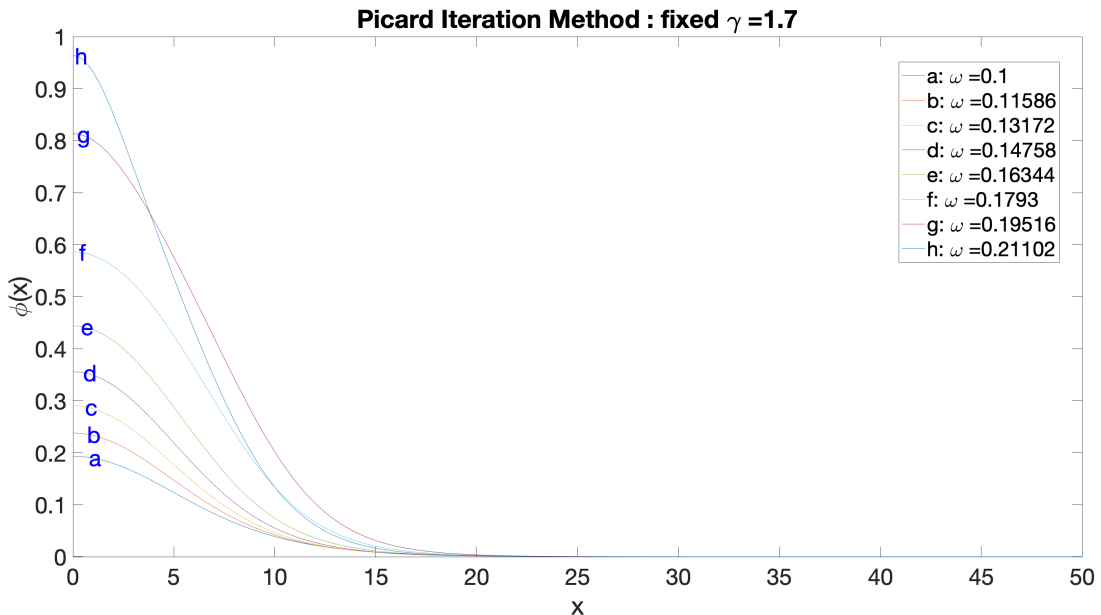


Figure 22: $\phi_{\omega,1.7}$ by Picard iteration method for fixed $\gamma = 1.7$ and several ω , with initial guess from shooting-cropping solutions and $dt = 0.1$.

We also computed the solutions for $\gamma = 1.8$ and several choices of ω . Note that $\gamma = 1.8$ is slightly greater than γ_1 and the pair (ω, γ) can be very close to Γ_{no} . The result is similar to what we get using Method 3 (see Figure 24), hence it is skipped.

We also computed the solutions for $\gamma = 10$ and several large values of ω . See Figure 23. The solutions are nice decaying functions with very compact supports. The computation ending time for Figure 23 is $T = 5$ for $dt = 0.01$ and 0.001 . Our other computations with $dt = 0.01$ and ending time $T = 50$ give similar results.

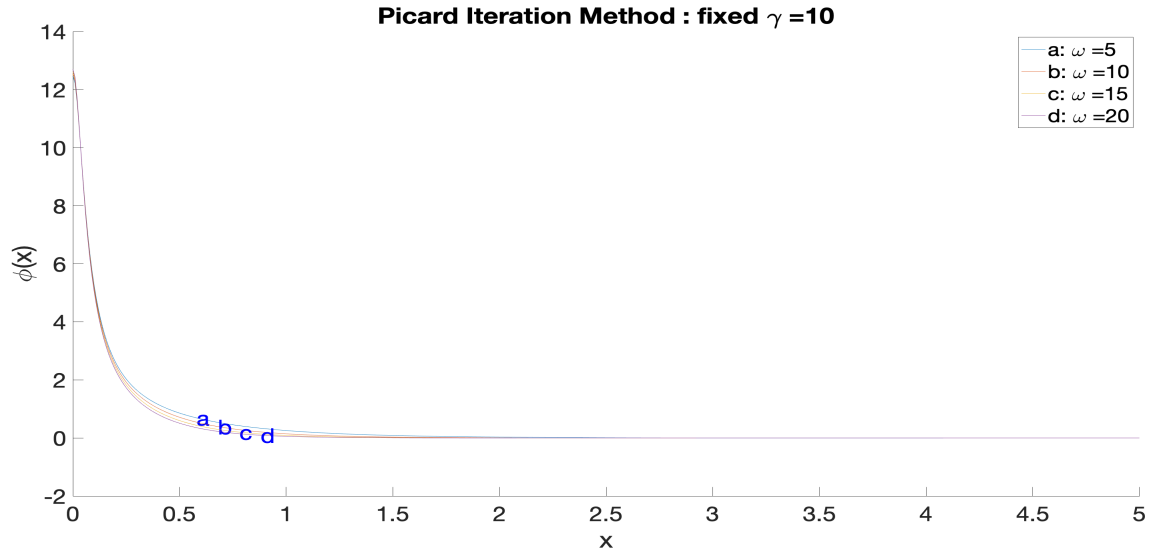


Figure 23: Picard iteration method for $\gamma = 10$ and $\omega = 5, 10, 15, 20$, with $dt = 0.01$ and the shooting-cropping solutions as initial guesses.

A difficulty with the Picard iteration method is that it takes a lot of computation power for smaller dt . When we take $dt = 0.001$, we need to shrink the time interval to at the largest $[0, 20]$ to compute it in a reasonable time.

5.3.3 MATLAB's `bvp4c` function method

Our third method is using the MATLAB function `bvp4c` to solve the ODE $\phi'' = g(\phi)$ given in (5.11) for $0 \leq t \leq 50$ subject to the boundary conditions (5.17). We use the shooting-cropping solution from Method 1 as the initial guess for the function `bvp4c`.

The numerical solutions obtained from Method 3 are usually nice looking monotonically decaying solutions. See Figure 24 for a few solutions by Method 3 for $\gamma = 1.8$.

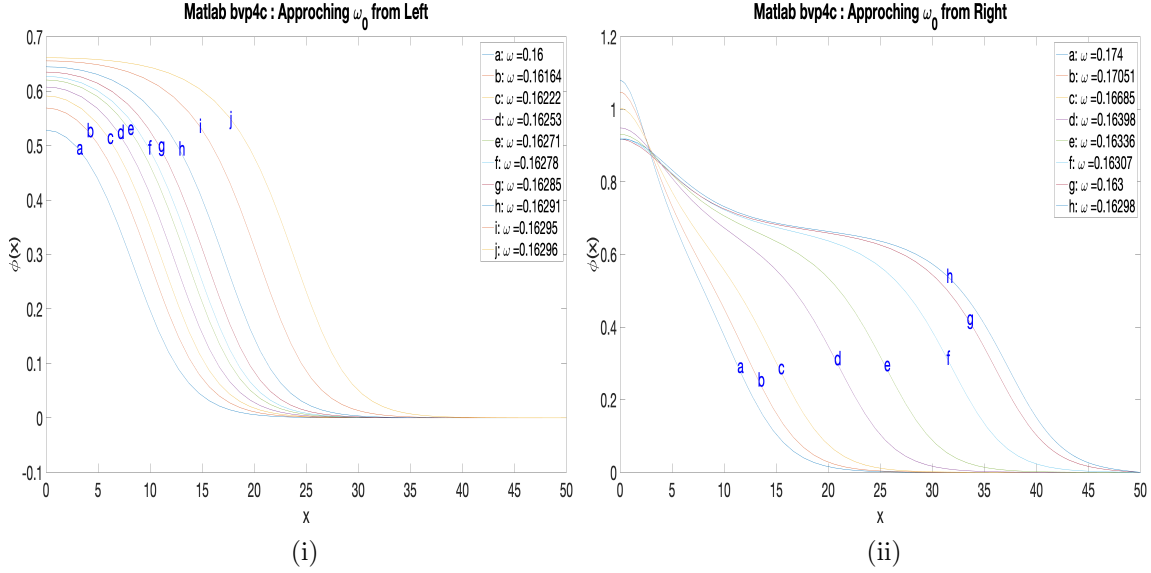


Figure 24: Method 3 for fixed $\gamma = 1.8$ for (i) $\omega < \omega_0$, (ii) $\omega > \omega_0$.

We also computed with Method 3 for $\gamma = 1.7$ and $\gamma = 10$. The results are similar to those obtained by Method 2, see Figures 22 and 23. Hence we skip the figures.

6 Appendix: Explicit formulas for standing waves

It is well known that the solution of

$$\phi_{xx} = \omega\phi - \phi^p, \quad (x \in \mathbb{R}) \quad (6.1)$$

for $1 < p < \infty$ is given by

$$\phi_{p,\omega}(x) = \omega^{1/(p-1)} Q_p(\omega^{1/2}x)$$

where $Q_p(x) = \phi_{p,1}(x)$ is given by

$$Q_p(x) = \left(\frac{p+1}{2} \operatorname{sech}^2 \left(\frac{p-1}{2}x \right) \right)^{\frac{1}{p-1}}$$

In the following we consider explicit solutions for double power nonlinearities. Let

$$v(x) = (\ell + \operatorname{ch}^2x)^{-\beta} \quad (6.2)$$

where $\ell \in (-1, \infty)$ and $\beta > 0$. Using $\operatorname{sh}^2 = \operatorname{ch}^2 - 1$, one gets $v_x(x) = -2\beta(\ell + \operatorname{ch}^2x)^{-\beta-1} \operatorname{ch}x \operatorname{sh}x$ and

$$v_{xx} = Av - Bv^{1+1/\beta} - Cv^{1+2/\beta},$$

where

$$A = 4\beta^2, \quad B = 2\beta(2\beta+1)(2\ell+1), \quad C = -4\beta(\beta+1)\ell(\ell+1).$$

To get double power nonlinearity we require $BC \neq 0$, i.e., $\ell \neq -1/2, 0$. There are three cases:

1. $\ell \in I_1 = (-1, -1/2)$: We have $B < 0$, $C > 0$, (defocusing-focusing, DF)
2. $\ell \in I_2 = (-1/2, 0)$: We have $B > 0$, $C > 0$, (focusing-focusing, FF)

3. $\ell \in I_3 = (0, \infty)$: We have $B > 0$, $C < 0$, (focusing-defocusing, FD)

Remark 6.1. The borderline cases $\ell = -1/2$ and $\ell = 0$ correspond to NLS with a focusing single power nonlinearity, and suggest that the profile of v near $\ell = -1/2$ and $\ell = 0$ are given by $Q_{1+1/\beta}$ and $Q_{1+2/\beta}$, respectively.

We now assume $\ell \neq -1/2, 0$ and denote $a_1 = \text{sgn } B$ and $a_2 = \text{sgn } C$. A suitable rescaling

$$\phi(x) = kv(\lambda x), \quad k = |C/B|^\beta, \quad \lambda = \frac{\sqrt{|C|}}{|B|}, \quad \omega = 4\beta^2 \lambda^2$$

gives a solution $\phi(x)$ of

$$\phi_{xx} = \omega\phi - a_1\phi^{1+1/\beta} - a_2\phi^{1+2/\beta}. \quad (6.3)$$

Explicitly,

$$\phi_\omega(x) = k \left(\ell + \text{ch}^2\left(\frac{\sqrt{\omega}}{2\beta}x\right) \right)^{-\beta}, \quad k = \left| \frac{2(\beta+1)\ell(\ell+1)}{(2\beta+1)(2\ell+1)} \right|^\beta,$$

and

$$\omega = \omega^* \frac{4|\ell|(\ell+1)}{(2\ell+1)^2}, \quad \omega^* = \frac{\beta(\beta+1)}{(2\beta+1)^2}. \quad (6.4)$$

Remark 6.2. Explicit solutions for (6.3) are well known. For example [24, (3.1)] has an equivalent formula for solutions of (6.3) with $a_1, a_2 \in \mathbb{R}$:

$$\phi_\omega(x) = \left(\frac{\omega}{A + \sqrt{A^2 + B\omega} \text{ch}(\beta^{-1}\sqrt{\omega}x)} \right)^\beta, \quad A = \frac{a_1}{2 + 1/\beta}, \quad B = \frac{a_2}{1 + 1/\beta}.$$

The main advantage of our form is the single parameter ℓ for all three cases: DF, FF and FD.

The original parameter ℓ can be solved in each interval I_j in terms of ω . Thus we can use ω as the parameter in each interval. Indeed, from (6.4), we have

$$\omega_{-1+} = 0, \quad \omega_{-1/2-} = \infty = \omega_{-1/2+}, \quad \omega_{0-} = 0 = \omega_{0+}, \quad \omega(\infty-) = \omega^*,$$

and

$$\frac{d\omega}{d\ell} = \frac{4\omega^* \text{sgn } \ell}{(2\ell+1)^3}$$

which is positive for $\ell \in (-1, -1/2) \cup (0, \infty)$, and negative for $\ell \in (-1/2, 0)$.

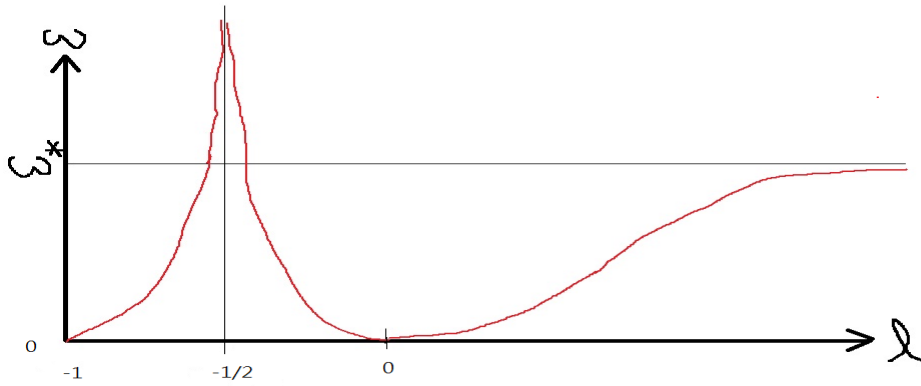


Figure 25: ω as a function of ℓ

Remark 6.3. Consider the limit $\ell = -1 + \varepsilon$ with $\varepsilon \rightarrow 0+$. We have $\omega \sim C\varepsilon$ and $\phi_\omega(x) \sim \phi_0(x) := c_1(c_2 + x^2)^{-\beta}$ for $|x| < \varepsilon^{-1/2}$ and $\phi_\omega(x) \sim c_3\varepsilon^\beta e^{-c_4\sqrt{\varepsilon}|x|}$ for $|x| > \varepsilon^{-1/2}$. It can be understood as the competition between $f(\phi)$ and $\omega\phi$ for $\omega \ll 1$. When $|f(\phi)| > \omega\phi$, i.e., when $|x| < \varepsilon^{-1/2}$, ϕ_ω is approximated by ϕ_0 , the solution of $\phi'' + f(\phi) = 0$. For $|x| > \varepsilon^{-1/2}$, $\omega\phi$ is larger than $f(\phi)$ and ϕ_ω is approximated the solution of $\phi'' = \omega\phi$. Similarly, we can consider the limits $\ell \rightarrow 0_-$ and $\ell \rightarrow 0_+$.

Acknowledgments

We warmly thank Vianney Combet for helpful discussions and continued interests in this work. We thank Stefan Le Coz for the reference [10]. We also thank the referee for very valuable suggestions. The work of Tsai was partially supported by NSERC grant RGPIN-2018-04137.

References

- [1] J. Angulo Pava and C. A. Hernández Melo. On stability properties of the cubic-quintic Schrödinger equation with δ -point interaction. *Commun. Pure Appl. Anal.*, 18(4):2093–2116, 2019.
- [2] J. Angulo Pava, C. A. Hernández Melo, and R. G. Plaza. Orbital stability of standing waves for the nonlinear Schrödinger equation with attractive delta potential and double power repulsive nonlinearity. *J. Math. Phys.*, 60(7):071501, 23, 2019.
- [3] H. Berestycki and P.-L. Lions. Nonlinear scalar field equations. I. Existence of a ground state. *Arch. Rational Mech. Anal.*, 82(4):313–345, 1983.
- [4] R. Carles, C. Klein, and C. Sparber. On soliton (in-)stability in multi-dimensional cubic-quintic nonlinear Schrödinger equations. *arXiv:2012.11637*, 2020.
- [5] T. Cazenave. *Semilinear Schrödinger equations*, volume 10 of *Courant Lecture Notes in Mathematics*. New York University, Courant Institute of Mathematical Sciences, New York; American Mathematical Society, Providence, RI, 2003.
- [6] V. Combet, T.-P. Tsai, and I. Zwiers. Local dynamics near unstable branches of NLS solitons. *arXiv:1207.0175*, 2012.
- [7] A. Comech, S. Cuccagna, and D. E. Pelinovsky. Nonlinear instability of a critical traveling wave in the generalized Korteweg-de Vries equation. *SIAM J. Math. Anal.*, 39(1):1–33, 2007.
- [8] A. Comech and D. Pelinovsky. Purely nonlinear instability of standing waves with minimal energy. *Comm. Pure Appl. Math.*, 56(11):1565–1607, 2003.
- [9] N. Fukaya. Instability of solitary waves for a generalized derivative nonlinear Schrödinger equation in a borderline case. *Kodai Math. J.*, 40(3):450–467, 2017.
- [10] N. Fukaya and M. Hayashi. Instability of algebraic standing waves for nonlinear Schrödinger equations with double power nonlinearities. 2020. <https://arxiv.org/abs/2001.08488>.
- [11] R. Fukuizumi. Remarks on the stable standing waves for nonlinear Schrödinger equations with double power nonlinearity. *Adv. Math. Sci. Appl.*, 13(2):549–564, 2003.

- [12] F. Genoud, B. A. Malomed, and R. M. Weishäupl. Stable NLS solitons in a cubic-quintic medium with a delta-function potential. *Nonlinear Anal.*, 133:28–50, 2016.
- [13] M. Grillakis, J. Shatah, and W. Strauss. Stability theory of solitary waves in the presence of symmetry. I. *J. Funct. Anal.*, 74(1):160–197, 1987.
- [14] M. Grillakis, J. Shatah, and W. Strauss. Stability theory of solitary waves in the presence of symmetry. II. *J. Funct. Anal.*, 94(2):308–348, 1990.
- [15] Z. Guo, C. Ning, and Y. Wu. Instability of the solitary wave solutions for the generalized derivative nonlinear Schrödinger equation in the critical frequency case. *Math. Res. Lett.*, 27(2):339–375, 2020.
- [16] I. D. Iliev and K. P. Kirchev. Stability and instability of solitary waves for one-dimensional singular Schrödinger equations. *Differential Integral Equations*, 6(3):685–703, 1993.
- [17] H. Kikuchi. Existence of standing waves for the nonlinear Schrödinger equation with double power nonlinearity and harmonic potential. In *Asymptotic analysis and singularities—elliptic and parabolic PDEs and related problems*, volume 47 of *Adv. Stud. Pure Math.*, pages 623–633. Math. Soc. Japan, Tokyo, 2007.
- [18] S. Le Coz, Y. Martel, and P. Raphaël. Minimal mass blow up solutions for a double power nonlinear Schrödinger equation. *Rev. Mat. Iberoam.*, 32(3):795–833, 2016.
- [19] M. Lewin and S. R. Nodari. The double-power nonlinear Schrödinger equation and its generalizations: uniqueness, non-degeneracy and applications. *arXiv:2006.02809*, 2020.
- [20] M. Maeda. Stability and instability of standing waves for 1-dimensional nonlinear Schrödinger equation with multiple-power nonlinearity. *Kodai Math. J.*, 31(2):263–271, 2008.
- [21] M. Maeda. Stability of bound states of Hamiltonian PDEs in the degenerate cases. *J. Funct. Anal.*, 263(2):511–528, 2012.
- [22] K. Nakanishi, T. V. Phan, and T.-P. Tsai. Small solutions of nonlinear Schrödinger equations near first excited states. *J. Funct. Anal.*, 263(3):703–781, 2012.
- [23] C. Ning. Instability of solitary wave solutions for the nonlinear Schrödinger equation of derivative type in degenerate case. *Nonlinear Anal.*, 192:111665, 23, 2020.
- [24] M. Ohta. Stability and instability of standing waves for one-dimensional nonlinear Schrödinger equations with double power nonlinearity. *Kodai Math. J.*, 18(1):68–74, 1995.
- [25] M. Ohta. Instability of bound states for abstract nonlinear Schrödinger equations. *J. Funct. Anal.*, 261(1):90–110, 2011.
- [26] M. Ohta and T. Yamaguchi. Strong instability of standing waves for nonlinear Schrödinger equations with double power nonlinearity. *SUT J. Math.*, 51(1):49–58, 2015.
- [27] J. Shatah and W. Strauss. Instability of nonlinear bound states. *Comm. Math. Phys.*, 100(2):173–190, 1985.